Practical Teleportation of an Unknown Quantum State

by

Syed Tahir Amin

A dissertation submitted in partial fulfillment of the requirements

for the degree of Master of Philosophy

in

Physics

Supervised by

Dr. Aeysha Khalique

School of Natural Sciences

National University of Sciences and Technology

Islamabad, Pakistan.

FORM TH-4

National University of Sciences & Technology

M.Phil THESIS WORK

We hereby recommend that the dissertation prepared under our supervision by: SYED TAHIR AMIN, Regn No. NUST201260312MCAMP78112F Titled: Practical Teleportation of an Unknown Quantum State be accepted in partial fulfillment of the requirements for the award of **M.Phil** degree.

Examination Committee Members

1. Name: Prof. Asghar Qadir Signature: Asghar Qadir

2. Name: Dr. Shahid Iqbal Signature:

3. Name: Dr. Manzoor Ikram Signature:

4. Name: Prof. Farhan Saif Signature:

Supervisor's Name: Dr. Aeysha Khalique Signature: Aeysha Khalique

Aeysha Khalique
Head of Department

6/2/15
Date

COUNTERSINGED

Date: 6/2/15

Dean/Principal

Abstract

Entanglement is the building block of different processes in quantum communication and quantum computation. We develop a theory to teleport an unknown quantum state using entanglement between two distant parties Aalia and Babar. Our theory takes into account experimental deficiencies due to contribution of multiphoton pair production of parametric down conversion source, inefficiency and dark counts of detectors and channel losses. We use a linear optics setup for teleportation of an unknown quantum state by performing Bell state measurement by the sender. Our theory successfully provides a model for experimentalists to optimize the fidelity by adjusting the experimental parameters. We apply our model to an experimental paper on quantum teleportation and the results obtained by our model using the parameters used in the experiment are perfectly in agreement with the experiment results.

Acknowledgement

In the name of 'ALLAH', the most gracious, the most merciful, the one and the only, the creator, *who is perfect in all characterization, worthy of worship. All praises be to Allah who guides us when we bewilder in darkness of ignorance and helps us in enlightening our ways.* Countless salutation to the source of knowledge Holy Prophet Muhammad (S.A.W), who declared it an obligatory duty of every Muslim to seek and acquire knowledge.

I wish to express my warmest, sincerest thanks and profound gratitude to my supervisor, Dr. Aeysha Khalique (HOD), Assistant Professor at School of Natural Science (SNS). It was because of his inspiring guidance, consistent encouragement, sympathetic attitude and dynamic supervision during the entire study program that enabled me to prepare this manuscript.

I am grateful to all of my teachers at School of Natural Sciences (SNS), National University of Sciences and Technology (NUST) because for their encouragement and inspiration.

I am sincerely thankful to all my friends and especially my class fellow Zainub Liaqat for their encouragement and nice company.

I wish to express my deepest gratitude to Mr. Asmat Amin, Mr. Mureed Hussian, Mr. Mehar Ali Malik, whose invaluable assistance enabled me to surmount this task.

At last but certainly not the least i would like to thank my family as it would have been impossible for me to accomplish this study without their incredible support. I am especially thankful to my parents, brothers and sisters for making me what i am today. In fact, it is the result of their love, affection and encouragement that kept me going.

Syed Tahir Amin

To My Parents And

Beloved Brother

Prof. Husnul Amin

Contents

Chapter 1

Introduction

In quantum information (QI), quantum mechanics manifest itself in a most profound way. Although basic principles of quantum mechanics were developed in the early twentieth century, yet it was only in the last two decades of twentieth century that quantum information protocols were developed based on these principles. These protocols involved quantum key distribution [1], quantum dense coding [2], quantum teleportation [3] and quantum error correction [4]. Various experiments have been performed to demonstrate these protocols using simple linear optics setups [5, 6, 7, 8]. The practical limitations of the resources effect the success of these experiments. There is a need to develop efficient model for these experiments so that optimal parameters of the resources can be predifined for an experiment. In this thesis we model quantum teleportation experiment taking into account various practical inefficiencies of the resources used.

In this chapter we cover some fundamentals mathematical concepts underlying our analysis of quantum teleportation. Section 1.1 explains some linear algebra underlying the quantum mechanical description of states. Then we discuss quantum states and quantum gates in Sec. 1.2. We explain the no-cloning theorem in Sec. 1.3. Section 1.4 is dedicated to sample spaces and probabilities. In Sec. 1.5 we provide a naive explanation of the quantum teleportation protocol. Finally in Sec. 1.6 we provide an outline of this thesis.

This experiment is performed with many different kinds of particles such as photons [10], neutrons [11], and atoms [12], and the same behavior as that of electrons [13], as discussed above, is observed.

Now we develop mathematical formulation and the underlying linear algebra of quantum systems in Sec. 1.1.

1.1 Quantum Systems and Linear Algebra

Quantum systems are physical systems which can be represented by Hilbert space. The dimensionality of the Hilbert space is decided by the ways in which that quantum system may be projected. i.e. in case of spin quantum system when we measured it gives either spin 'up' or 'down' . So this quantum system has two allowed paths, therefore this system belongs to two dimensional Hilbert space. Here we briefly discuss some important linear algebra with some emphasis on Hermitian matrices. Suppose a Hilbert Space (H) of finite dimensionality 'k' such that vector $|a\rangle, |b\rangle \in H$. Then the inner (Hermitian) product of these two vectors

$$|a\rangle = \begin{pmatrix} a_1 \\ a_2 \\ . \\ . \\ a_k \end{pmatrix}, \quad |b\rangle = \begin{pmatrix} b_1 \\ b_2 \\ . \\ . \\ b_k \end{pmatrix}, \langle a| = (|a\rangle)^\dagger = \begin{pmatrix} \bar{a}_1 \ \bar{a}_2 .. \ \bar{a}_k \end{pmatrix}, \tag{1.1}$$

is given as

$$\langle a|b\rangle = \bar{a_1}b_1 + \bar{a_2}b_2 + ... + \bar{a_k}b_k := \sum_{i=1}^{k} \bar{a_i}b_i \in \mathbb{C}, \tag{1.2}$$

where $\bar{z}$ is the complex conjugate of a complex number 'z'. In order to normalize any vector, we generally divide it by its norm, $||z|| := \sqrt{\langle z|z\rangle}$. It should be noted that the Cauchy-Schwarz inequality ($\|a\|\|b\| \geq \|\langle a|b\rangle\|$) must be satisfied by the inner product. Consider the following matrix A

$$A = \begin{pmatrix} a_{1,1} \ a_{1,2} \ \dots \ a_{1,k} \\ a_{2,1} \ a_{2,2} \ \dots \ a_{2,k} \\ \vdots \ \vdots \ \ddots \ \vdots \\ a_{k,1} \ a_{k,2} \ \dots a_{k,k} \end{pmatrix}. \tag{1.3}$$

We then define the transpose (A^T) and the complex conjugate ($\bar{A}$) of matrix as

$$A^T = \begin{pmatrix} a_{1,1} \ a_{2,1} \ \dots \ a_{k,1} \\ a_{1,2} \ a_{2,2} \ \dots \ a_{k,2} \\ \vdots \ \vdots \ \ddots \ \vdots \\ a_{1,k} \ a_{2,k} \ \dots a_{k,k} \end{pmatrix}, \quad \bar{A} = \begin{pmatrix} \bar{a}_{1,1} \ \bar{a}_{1,2} \ \dots \ \bar{a}_{1,k} \\ \bar{a}_{2,1} \ \bar{a}_{2,2} \ \dots \ \bar{a}_{2,k} \\ \vdots \ \vdots \ \ddots \ \vdots \\ \bar{a}_{k,1} \ \bar{a}_{k,2} \ \dots \bar{a}_{k,k} \end{pmatrix}. \tag{1.4}$$

Now for any matrix to be Hermitian it must satisfies the following condition,

$$A = A^\dagger = \begin{pmatrix} \bar{a}_{1,1} & \bar{a}_{2,1} & \dots & \bar{a}_{k,1} \\ \bar{a}_{1,2} & \bar{a}_{2,2} & \dots & \bar{a}_{k,2} \\ \vdots & \vdots & \ddots & \vdots \\ \bar{a}_{1,k} & \bar{a}_{2,k} & \dots & \bar{a}_{k,k} \end{pmatrix}, \tag{1.5}$$

where $A^\dagger = \bar{A}^T$. Also this Hermitian matrix A is called positive semidefinite denoted by $A \geq 0$ if for an arbitrary vector $c \in H$, it satisfies the relation $\langle c|Ac\rangle \geq 0$. For non zero vector '$c$' , if $\langle c|Ac\rangle > 0$, then A is positive definite. If we first diagonalize matrix A, then the condition of positive semi-definiteness tells us that eigen values of matrix A are either zero or positive.

Hermitian inner product can also be obtained as the matrix multiplication of $\langle c|$ and $|c\rangle$. Working in Bra-Ket notation for any matrix A, $|Ac\rangle = A|c\rangle, \langle Ac| = \langle c|A^\dagger$. For Hermitian matrix A we get $\langle a|Ab\rangle = \langle Aa|b\rangle$ also equals $\mathrm{Tr}|b\rangle\langle a|A$. We also define for some matrices A and B, the symmetrized and commutator relation.

$$\{A, B\} := \frac{1}{2}(AB + BA), \tag{1.6}$$

$$[A, B] := \frac{1}{2}(AB - BA). \tag{1.7}$$

A vector space is called a Jordan or Lie algebra if it is closed under Eq. (1.6) or (1.7) respectively.

1.2 Quantum States and Quantum Gates

We now explain various aspects of quantum states. In Sec. 1.2.1 we give a description of quantum bit. Section 1.2.2 explains composite systems and its tensor products. Then we discuss quantum gates in Sec. 1.2.3. In Sec. 1.2.4 we covers two particle states and its different types and behavior.

1.2.1 Qubit

The basic unit for information science is bit, which can take one of the two possible values '0' and '1'. Classical realization of a bit, may be imagined as a mechanical switch, which is designed to have two distinct states, with sufficient large energy barrier between them so

that no spontaneous transition can occur between the two states. In QI theory the basic unit of information is qubit, short for quantum bit, which is two state quantum system, where the two states are $|0\rangle$ and $|1\rangle$. So any quantum system with at least two states can serve as qubit, many of which have already been experimentally realized, i.e. spin of electron, polarization of photon etc.

According to quantum mechanics qubit can also be in the superposition of these states, so generally qubit can be written in Dirac or Bra-Ket notation as

$$|\varphi\rangle \quad = \quad \alpha|0\rangle + \beta|1\rangle, \tag{1.8}$$

where α and β are complex numbers. For a normalized state these complex numbers must obey $|\alpha|^2+|\beta|^2 = 1$. These complex numbers are also known as probability amplitudes and the square of probability amplitude is called probability. Since we know that probability of certain events always sum up to 1, thats why the sum of $|\alpha|^2$ and $|\beta|^2$ gives one. It should be noted that Eq. (1.8), does not mean that the state of qubit is somewhere between '0' and '1', but it shows that qubit is in superposition of both states, and if we measure it, we will find out qubit in state $|0\rangle$ with probability $|\alpha|^2$ and in state $|1\rangle$ with probability $|\beta|^2$.

To specify any qubit, we just need two complex variable α and β. On the other hand using coordinate representation qubit state (1.8) is written as.

$$|\varphi\rangle = \begin{pmatrix} \alpha \\ \beta \end{pmatrix}, \tag{1.9}$$

with $|0\rangle = \begin{pmatrix} 1 \\ 0 \end{pmatrix}$ and $|1\rangle = \begin{pmatrix} 0 \\ 1 \end{pmatrix}$. Bra-Ket notation and coordinate representation are the two sides of a same coin, means that sometimes it is easy to solve a problem by using coordinate representation than the Bra-Ket notation and vise versa. In quantum systems, the description of the current condition of that system, such as the polarization, is known as *state*. So we can also equally describe any state by a Hermitian matrix ρ known as density operator or density matrix, and mathematically given as

$$\rho = \sum_i \quad p_i|\psi_i\rangle\langle\psi_i|, \tag{1.10}$$

if one of the all probabilities is one i.e., if $p_i = \delta_{ij}$, then the above density operator reduces to simple form $\rho = |\psi_i\rangle\langle\psi_i|$. Such operator for which the state vector is known are called *pure states or pure state density operators*. These operators are obtained by taking outer product of state vector with it self. On the other hand the density matrix in Eq. (1.10) with any probability not equal to one generally represents a statistical mixture of states or mixed state.

1.2.2 Composite Systems and Tensor Products

Suppose we have two quantum systems belonging to Hilbert spaces H_A and H_B with orthogonal basis $\{a_1, a_2, a_3, ..., a_d\}$ and $\{b_1, b_2, b_3, ..., b_d\}$ respectively. Then any combined system of H_A and H_B is called composite system. The Hilbert space of composite system is given by the tensor product of Hilbert spaces H_A and H_B as $H_A \otimes H_B$ with orthonormal basis $\{a_1 \otimes b_1, a_1 \otimes b_2, a_1 \otimes b_3, ..., a_1 \otimes b_d, a_2 \otimes b_1, a_2 \otimes b_2, a_2 \otimes b_3, ..., a_2 \otimes b_d, ..., a_d \otimes b_1, a_d \otimes b_2, a_d \otimes b_3, ..., a_d \otimes b_d\}$. This composite system has dimension $d \times d$. The tensor product of two vectors $x = \sum_i c^i |a_i\rangle$ and $y = \sum_j c^{'j} |b_j\rangle$ is given as

$$|x \otimes y\rangle \quad = \quad \sum_{i,j} c^i c^{'j} |a_i\rangle \otimes |b_j\rangle, \tag{1.11}$$

or we can simply omit '$\otimes$ ' from the above equation,

$$|xy\rangle \quad = \quad \sum_{i,j} c^i c^{'j} |a_i b_j\rangle. \tag{1.12}$$

Now if we have two operators in the form of matrices, i.e. X^A on H_A and X^B on H_B then the tensor product $X^A \otimes X^B$ on combine Hilbert space is defined as

$$X^A \otimes X^B(|a_i\rangle \otimes |b_j\rangle) \quad = \quad X^A|a_i\rangle \otimes X^B|b_j\rangle, \tag{1.13}$$

where, $|a_i\rangle(|b_j\rangle)$ are orthonormal basis of Hilbert spaces $H_A(H_B)$, respectively. Furthermore trace of tensor product $X^A \otimes X^B$ satisfies the relation

$$Tr(X^A \otimes X^B) \quad = \quad TrX^A TrX^B.$$

For any number of Hermitian matrices for instant X^A, Y^A and Z^A on Hilbert space H_A, and X^B, Y^B and Z^B on Hilbert space H_B, we have

$$(X^A \otimes X^B)(Y^A \otimes Y^B)(Z^A \otimes Z^B) \quad = \quad (X^A Y^A Z^A) \otimes (X^B Y^B Z^B),$$

it follows from above equation

$$Tr(X^A \otimes X^B)(Y^A \otimes Y^B)(Z^A \otimes Z^B) \quad = \quad Tr(X^A Y^A Z^A) \otimes Tr(X^B Y^B Z^B).$$

After we have basic knowledge of quantum state, its time to discuss how states evolve. In following section we explain quantum gates which transform state of a system from some initial to final state.

Figure 1.1: General one qubit gate.

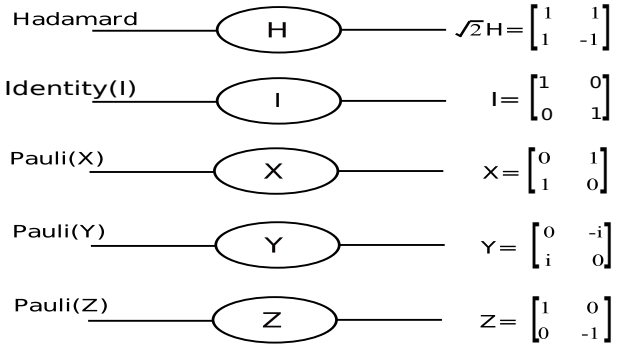

Figure 1.2: Fundamental one qubit gates, with there unitary transformation matrices.

1.2.3 Quantum Gates

In QI, the orthogonal qubit states $|0\rangle$ and $|1\rangle$ are substituted in place of classical logical values 0 and 1. Thus we have a large number of allowed states in the form of superposition of $|0\rangle$ and $|1\rangle$. Since action of any unitary transformation on a qubit is allowed by quantum mechanics, therefore a device which unitary transform qubit in a controlled manner is called qubit gate. Left hand side of Fig. 1.1 shows the initial state ($|\phi\rangle$), which then transformed into ($U|\phi\rangle$) shown on right side by one qubit gate 'U'. Among the throng of all possible one qubit quantum gate, there are some one qubit quantum gates, which are of fundamental importance. These single qubit gates are building blocks of all other quantum gates. Fig. 1.2 shows the most fundamental gates, the Hadamard, Pauli (X,Y,Z) and phase along with their unitary transformation in matrix form. In Dirac notation (Bra-Ket), these one qubit quantum gates can be written as

$$H = \frac{1}{\sqrt{2}}(|0\rangle + |1\rangle)\langle 0| + \frac{1}{\sqrt{2}}(|0\rangle - |1\rangle)\langle 1|, \tag{1.14}$$

$$I = |0\rangle\langle 0| + |1\rangle\langle 1|, \tag{1.15}$$

$$X = |1\rangle\langle 0| + |0\rangle\langle 1|, \tag{1.16}$$

$$Y = i|1\rangle\langle 0| - i|0\rangle\langle 1|, \tag{1.17}$$

$$Z = |0\rangle\langle 0| - |1\rangle\langle 1|. \tag{1.18}$$

Figure 1.3: Hydrogen atom as Qubit

The Paul (X) gate is also known as NOT gate or flip gate because this gate converts quantum states $|0\rangle$ and $|1\rangle$ into $|1\rangle$ and $|0\rangle$ respectively. In Dirac notation we can write CNOT gate transformation as

$$CNOT = |00\rangle\langle 00| + |01\rangle\langle 01| + |11\rangle\langle 10| + |10\rangle\langle 11|. \tag{1.19}$$

CNOT gate when act on two particle quantum states, it takes state of first qubit as control qubit and change the state of second qubit from $|0\rangle$ to $|1\rangle$ and vice versa, if the first qubit is in state $|1\rangle$. On the other hand if the first qubit state is $|0\rangle$ then it does not change the state of second qubit.

1.2.4 Separable and Entangled States

Suppose we have two qubits A and B which are represented by hydrogen atom, whose ground state represents $|0\rangle$ and excited state represents $|1\rangle$ as shown in Fig. 1.3. Lets take first and the second qubit in the states

$$\phi_A = a_0|0\rangle + a_1|1\rangle, \tag{1.20}$$
$$\phi_B = b_0|0\rangle + b_1|1\rangle. \tag{1.21}$$

We are going to find out the composite state of above two states which is obtained simply by taking tensor product of Eqs. (1.20) and (1.21)

$$\begin{aligned} \phi_A \otimes \phi_B &= (a_0|0\rangle + a_1|1\rangle) \otimes (b_0|0\rangle + b_1|1\rangle, \\ &= a_0b_0|00\rangle + a_1b_0|10\rangle + a_0b_1|01\rangle + a_1b_1|11\rangle. \end{aligned} \tag{1.22}$$

Any quantum state which can be written as a product of individual systems is separable and one which cannot be written in product form is entangled.

Now suppose we have a composite system which is in equal superposition of $|00\rangle$ and $|11\rangle$ given in Eq. (1.29)

$$|\phi^+\rangle_{AB} = \frac{1}{\sqrt{2}}(|00\rangle + |11\rangle)_{AB}. \tag{1.23}$$

Above quantum state is entangled state and it is impossible to factor it out as product of individual quantum state of particles. Using the method of proof, known as *proof by contradiction*, we suppose that it is possible to factor the above equation as product of quantum states of individual quantum systems.

$$\begin{aligned} |\phi^+\rangle_{AB} &= (a_0|0\rangle + a_1|1\rangle)_A(b_0|0\rangle + b_1|1\rangle)_B, \\ &= a_0b_0|00\rangle + a_1b_0|10\rangle + a_0b_1|01\rangle + a_1b_1|11\rangle. \end{aligned} \tag{1.24}$$

Comparing coefficient of Eqs. (1.23) and (1.24) we get

$$a_0b_0 = \frac{1}{\sqrt{2}}, \quad a_1b_0 = 0, \quad a_0b_1 = 0, \quad a_1b_1 = \frac{1}{\sqrt{2}}, \tag{1.25}$$

which is impossible, because if $a_1b_0 = 0$ which shows that either $a_1 = 0$ or $b_0 = 0$ or both be zero. Let us take, for instance, that $a_1 = 0$ and $b_0 \neq 0$, then a_1b_1 must equals to zero, but in entangled state given above this product of amplitudes is $a_1b_1 = \frac{1}{\sqrt{2}}$, which is contradictory. In short, the first and fourth term of Eq. (1.25) suggest that a_0, a_1, b_0, $b_1 \neq 0$, where the second and third term suggest that either all amplitude a_0, a_1, b_0, $b_1 = 0$ or at least some of them must be zero, which is impossible. Therefore Eq. (1.23) is the state of two qubits which cannot be written as the tensor product of states of individual qubits A and B, and the two qubits are inherently entangled with each other.

In order to further explain the difference between separable and entangled state; suppose we have two quantum systems from Hilbert spaces H_A and H_B, whose states are represented by ρ_A and ρ_B, which are totally independent of each other. Then the tensor product $\rho_A \otimes \rho_B$ of density matrices represents the state of composite system. Such a state is called *tensor product state*. On the composite system $H_A \otimes H_B$, there are some density matrices ρ which can be written as a probabilistic mixture of tensor product states known as decomposable or separable states

$$\rho = \sum_j \lambda_j \rho_A^j \otimes \rho_B^j, \quad \lambda_j \geq 0, \quad \sum_j \lambda_j = 1. \tag{1.26}$$

Quantum states represented by Eq. (1.26) lack very interesting property known as entanglement. Interesting thing about the behavior of entangled quantum systems is that

when we measure one quantum system the other quantum system always project on subspace which entanglement predicts. In case of two particle quantum system H_A and H_B represented as tensor product $H_A \otimes H_B$. In two particle system we have four maximally entangled states,

$$|e^1\rangle_{AB} = |\psi^+\rangle_{AB} = \frac{1}{\sqrt{2}}(|01\rangle + |10\rangle)_{AB}, \tag{1.27}$$

$$|e^2\rangle_{AB} = |\psi^-\rangle_{AB} = \frac{1}{\sqrt{2}}(|01\rangle - |10\rangle)_{AB}, \tag{1.28}$$

$$|e^3\rangle_{AB} = |\phi^+\rangle_{AB} = \frac{1}{\sqrt{2}}(|00\rangle + |11\rangle)_{AB}, \tag{1.29}$$

$$|e^4\rangle_{AB} = |\phi^-\rangle_{AB} = \frac{1}{\sqrt{2}}(|00\rangle - |11\rangle)_{AB}. \tag{1.30}$$

Above four states are also known as Bell states. It is important to note that above states also span the four dimensional Hilbert space of two quantum system because they are orthonormal states i.e.,

$$\langle e^i|e^j\rangle_{AB} = \delta_{i,j}. \tag{1.31}$$

It means that we can represent any two particles quantum state in terms of basis $\{|00\rangle, |01\rangle, |10\rangle, |11\rangle\}$ and $\{|e^1\rangle, |e^2\rangle, |e^3\rangle, |e^4\rangle\}$ equally likely.

Entanglement Generation and Some Properties of Bell States

Bell states which are maximally entangled two particle quantum states can be generated by first using Hadamard quantum operator on first qubit and then CNOT-gate taking first qubit as control bit of some initial state $|ij\rangle_{AB}$, where i,j $\in$ {0,1}.

To generate $|\phi^+\rangle_{AB}$ we take both $i = j = 0$,and then apply the above procedure i.e.,

$$|00\rangle_{AB} \xrightarrow{H_A} \frac{1}{\sqrt{2}}(|00\rangle + |10\rangle)_{AB} \xrightarrow{CNOT_{A=\text{control bit}}} \frac{1}{\sqrt{2}}(|00\rangle + |11\rangle)_{AB} = |\phi^+\rangle_{AB}. \tag{1.32}$$

Similarly for other three Bell state follow the same procedure but with different values of 'i' and 'j' in initial state $|ij\rangle$ shown in Fig. 1.4. For $|\phi^-\rangle_{AB}$ we took initial value $i = 1$ and $j = 0$ as

$$|10\rangle_{AB} \xrightarrow{H_A} \frac{1}{\sqrt{2}}(|00\rangle - |10\rangle)_{AB} \xrightarrow{CNOT_{A=\text{control bit}}} \frac{1}{\sqrt{2}}(|00\rangle - |11\rangle)_{AB} = |\phi^-\rangle_{AB}. \tag{1.33}$$

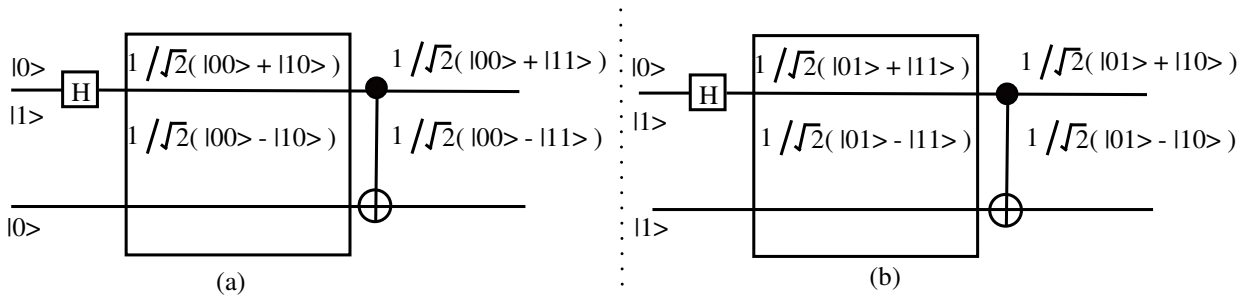

Figure 1.4: Bell state Generation

To generate $|\psi^+\rangle_{AB}$, $i = 0$ and $j = 1$

$$|01\rangle_{AB} \xrightarrow{H_A} \frac{1}{\sqrt{2}}(|01\rangle + |11\rangle)_{AB} \xrightarrow{CNOT_{A=\text{control bit}}} \frac{1}{\sqrt{2}}(|01\rangle + |10\rangle)_{AB} = |\psi^+\rangle_{AB}. \quad (1.34)$$

Similarly for $|\psi^-\rangle_{AB}$ we have

$$|11\rangle_{AB} \xrightarrow{H_A} \frac{1}{\sqrt{2}}(|01\rangle - |11\rangle)_{AB} \xrightarrow{CNOT_{A=\text{control bit}}} \frac{1}{\sqrt{2}}(|01\rangle - |10\rangle)_{AB} = |\psi^-\rangle_{AB}. \quad (1.35)$$

Rotational Invariance of Bell State

Here we want to discuss the very important property of Bell states. Their rotational invariance, which means that either using $\{|0\rangle, |1\rangle\}$ or any other orthonormal basis, the shape of Bell state can't change. For example take $|\phi^+\rangle$ in $\{|0\rangle, |1\rangle\}$ basis,

$$|\phi^+\rangle = \frac{1}{\sqrt{2}}(|00\rangle + |11\rangle). \quad (1.36)$$

Now rotating above state by 45 degree angle, which means that $\{|0\rangle, |1\rangle\}$ changes to sign basis $\{|+\rangle, |-\rangle\}$ as follow

$$|0\rangle = \frac{1}{\sqrt{2}}(|+\rangle + |-\rangle),$$
$$|1\rangle = \frac{1}{\sqrt{2}}(|+\rangle - |-\rangle), \quad (1.37)$$

putting values of $|0\rangle$ and $|1\rangle$ from Eq. (1.37) in Eq. (1.36)

$$|\phi^+\rangle = \frac{1}{\sqrt{2}}(\frac{1}{\sqrt{2}}(|+\rangle + |-\rangle)\frac{1}{\sqrt{2}}(|+\rangle + |-\rangle) + \frac{1}{\sqrt{2}}(|+\rangle - |-\rangle)\frac{1}{\sqrt{2}}(|+\rangle - |-\rangle)),$$

$$|\phi^+\rangle = \frac{1}{\sqrt{2}}(\frac{1}{2}(|++\rangle + |-+\rangle) + |+-\rangle + |--\rangle) + \frac{1}{2}(|++\rangle - |-+\rangle + |--\rangle - |+-\rangle),$$

$$|\phi^+\rangle = \frac{1}{\sqrt{2}}(|++\rangle + |--\rangle). \tag{1.38}$$

Now taking any general orthonormal basis as

$$|w\rangle = a_0|0\rangle + a_1|1\rangle \quad \text{and} \quad |w^\perp\rangle = a_1|0\rangle - a_0|1\rangle, \tag{1.39}$$

with $|a_0|^2 + |a_1|^2 = 1$. To show rotational invariance of Bell state, we finally suppose that Bell state (1.36), in basis $\{|w\rangle, w^\perp\rangle\}$ can be written as

$$|\phi^+\rangle = \frac{1}{\sqrt{2}}(|ww\rangle + |w^\perp w^\perp\rangle). \tag{1.40}$$

To show that Eq. (1.40) is equal to Eq. (1.36), we simply put values of $|w\rangle/|w^\perp\rangle$ from Eq. (1.39) into Eq. (1.40)

$$\begin{aligned}
|\phi^+\rangle &= \frac{1}{\sqrt{2}}((a_0|0\rangle + a_1|1\rangle)(a_0|0\rangle + a_1|1\rangle) + (a_1|0\rangle - a_0|1\rangle)(a_1|0\rangle - a_0|1\rangle)),\\
|\phi^+\rangle &= \frac{1}{\sqrt{2}}(|a_0|^2|00\rangle + a_0a_1|10\rangle + a_0a_1|01\rangle + |a_1|^2|11\rangle)\\
&\quad +(|a_1|^2|00\rangle - a_0a_1|10\rangle - a_0a_1|01\rangle + |a_0|^2|11\rangle),\\
|\phi^+\rangle &= \frac{1}{\sqrt{2}}((|a_0|^2 + |a_1|^2)|00\rangle + (|a_0|^2 + |a_1|^2)|11\rangle).
\end{aligned}$$

Using condition from Eq. (1.39),

$$|\phi^+\rangle = \frac{1}{\sqrt{2}}(|00\rangle + |11\rangle). \tag{1.41}$$

So Bell state can be written in any orthonormal basis which spans 2 dimensional Hilbert space.

$$|\phi^+\rangle = \frac{1}{\sqrt{2}}(|00\rangle + |11\rangle) = \frac{1}{\sqrt{2}}(|++\rangle + |--\rangle) = \frac{1}{\sqrt{2}}(|ww\rangle + |w^\perp w^\perp\rangle). \tag{1.42}$$

Rotational invariance of Bell states is very important to study the non-classical correlation in quantum systems.

1.3 No-Cloning Theorem

In 1982 Wootters and Zurek [23] published a theorem known as no-cloning theorem which state that it is impossible to perfectly clone non-orthonormal quantum states. To explain this theorem suppose we have some unitary operator as a copying machine which copies orthogonal states $|0\rangle/|1\rangle$ on some state $|a\rangle$ as

$$U|0\rangle|a\rangle = |0\rangle|0\rangle, \tag{1.43}$$
$$U|1\rangle|a\rangle = |1\rangle|1\rangle. \tag{1.44}$$

Now we want to use this unitary machine to copy a superposition state of the form $\alpha|0\rangle + \beta|1\rangle$

$$\begin{aligned} U(\alpha|0\rangle + \beta|1\rangle)|a\rangle &= \alpha U|0\rangle|a\rangle + \beta U|1\rangle|a\rangle = \alpha|0\rangle|0\rangle + \beta|1\rangle|1\rangle \\ &\neq (\alpha|0\rangle + \beta|1\rangle)(\alpha|0\rangle + \beta|1\rangle). \end{aligned} \tag{1.45}$$

So it is clear from above calculation that it is impossible to copy or clone non orthonormal quantum states. This theorem suggests that if one wants to send quantum state from one place to another, the quantum particle whose state we want to teleport must be destroyed completely in order to get exactly the same replica at the receiver lab. Therefore any quantum teleportation scheme must satisfy this theorem.

1.4 Sample Space, Probability and Baye's Theorem

Sample space is the set of all possible out comes of an experiment which may be discrete or continuous and finite. For example we take two dies each has six sides and we roll them performing a probabilistic experiment. The sample space of this experiment is shown in Fig. 1.5. So each time we roll both dies, we get a pair of numbers and each one of the possible pair of numbers corresponds to the little square of sample space shown in Fig. 1.5. In this case we have total 36 outcomes. Since we define that sample space as a set of outcomes of an experiment, then any subset of this sample space is called an event. It should be noted that probabilities are assigned to the events of a finite sample space and defined as

$$\text{Probability of an event happening in an experiment} = \frac{\text{Number of ways the event can happen}}{\text{Total number of outcomes of an experiment}}.$$

Consider an unbiased coin, which has sample space given by set {H,T} which has total number of outcomes two, then the probability of event head (tail) represented as $p(H)$ $(p(T))$ respectively given as

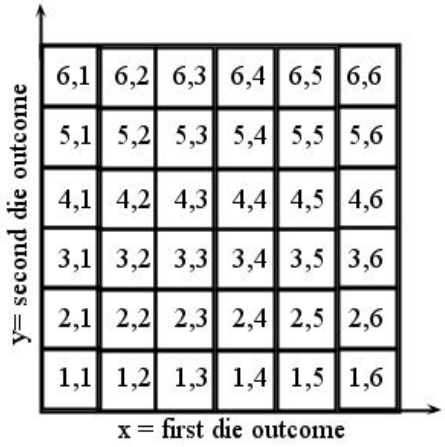

Figure 1.5: Sample space

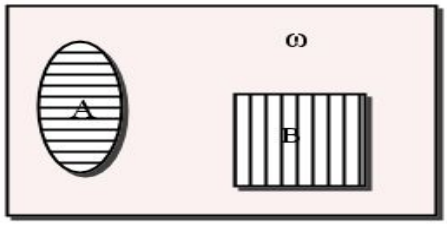

Figure 1.6: Sample space 'ω' with subsets 'A' and 'B'

Probability of head (tail)= $\frac{\text{Number of ways head (tail) can happen}}{\text{Total number of outcomes}} = \frac{1}{2}$.

Now we are going to discuss some fundamental axioms of probability, for this purpose let us take a sample space 'ω' with subset 'A' and 'B' with probabilities $p(A)$ and $p(B)$ respectively as shown in Fig. 1.6. Then we have following axioms of probability

- $Non - negativity : p(A) \geq 0$,
- Normalization condition : $p(\omega) = 1$,
- For any two disjoint events A and B i.e. $A \cap B = \emptyset$ then : $p(AUB) = P(A) + P(B)$.

Above axioms suggest that probability of any event can never be negative and that the probability of any event of probabilistic experiment must belong from the sample space of that experiment.

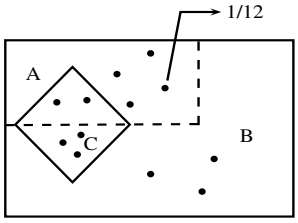

Figure 1.7: Sample space with subsets 'A', 'B' and 'C'

Bayesian inference is a type of inference which is used to update probabilities. Consider two events with probability $p(A)$ and $p(B)$, then we can update our probability of event A such that event B has already occurred as

$$p(A|B) = \frac{p(A \cap B)}{p(B)} = \frac{p(B|A)p(A)}{p(B)}. \tag{1.46}$$

We explain Bayesian inference with the following examples.

- *Example* :: 1

Consider a sample space consisting of three subset 'A', 'B' and 'C' with probabilities $p(A)$, $p(B)$ and $p(C)$ respectively as shown in Fig. 1.7. There are twelve equally likely outcomes, each with probability '$\frac{1}{12}$' . Probabilities that events 'A' and 'C' will happen are given as

$$p(A) = \frac{6}{12} = \frac{1}{2}, \tag{1.47}$$

$$p(C) = \frac{5}{12}. \tag{1.48}$$

If we are given that already event 'A' has happened then what will be the probability that event 'C' will happen. To find probability such that we are given some prior probability we use Bayesian inference

$$p(C|A) = \frac{p(A \cap C)}{p(A)} = \frac{\frac{2}{12}}{\frac{6}{12}} = \frac{1}{3}. \tag{1.49}$$

So by using Bayesian inference we update our previous probability of event 'C' .

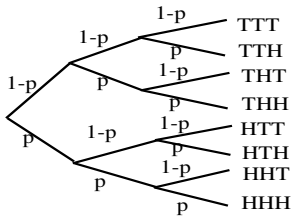

Figure 1.8: Sample space of a biased coin tossed three times, with probability of having head, $p(H) = p$ and probability of having tail is $p(T) = 1 - p$

- *Example* :: 2

In this example we take a biased coin with probability of having head $p(H) = p$ and probability of having tail is $p(T) = 1 - p$ as shown in the Fig. 1.8. Now tossing this biased coin three times, we note that the combine outcome must belong to the sample space consist of eight outcomes as shown in Fig. 1.8, i.e. $\{TTT, TTH, THT, THH, HTT, HTH, HHT, HHH\}$. First finding out some prior probabilities and then using Bayesian rule, we will find out conditional probability of certain event.

$$\begin{aligned} p(1 \text{ head}) &= p(HTT) + p(THT) + p(TTH) \\ &= p(1-p)(1-p) + (1-p)p(1-p) + (1-p)(1-p)p = 3p(1-p)^2. \end{aligned} \tag{1.50}$$

Using Bayesian inference to find out what will be the probability of outcome having first toss head such that events with only one head already have happened i.e.

$$\text{p(first toss is head}|1 \text{ head}) = \frac{p(1 \text{ head } \cap \text{first toss is head})}{p(1 \text{ head })} = \frac{p(1-p)^2}{3p(1-p)^2} = \frac{1}{3}. \tag{1.51}$$

- *Example* :: 3

Consider a six sided die with each side having equal probability i.e., $p(\text{each side}) = \frac{1}{6}$. If we throw the die, the probability of coming side 4 is $p(4) = \frac{1}{6}$. Now the probability of event other than four $\bar{p}(4)$ is just obtained by subtracting $p(4)$ from one as

$$\bar{p}(4) = 1 - p(4) = 1 - \frac{1}{6} = \frac{5}{6} \tag{1.52}$$

Well, now throw the same die twice, then what will be the probability that at least 4, will happen. To find this probability, we have two methods, first one is to count the outcome pair which consist of at least 4, and then divide this number by total number of out come pairs, looking at the Fig. (1.5), we can write

$$p(\text{atleast one 4 happens}) = \frac{\text{total number of outcome having atleast one 4}}{\text{total number of outcome}} = \frac{11}{36}. \quad (1.53)$$

Second method is to use the formula given below

$$\begin{aligned} p(\text{any side of die at least once}) \quad = \quad & 1 \\ & -(1 - p(\text{that side to happen when we throw die first time}))^i, \\ & \text{where i= number times the die thrown.} \end{aligned} \quad (1.54)$$

So for a die to throw it twice , $i = 2$, now to find the probability for 4 at least happen, we use above equation

$$p(4 \text{ least once}) = 1 - (1 - p(4))^2 = 1 - (1 - \frac{1}{6})^2 = 1 - (\frac{5}{6})^2 = 1 - \frac{25}{36} = \frac{11}{36} \quad (1.55)$$

In our theory of measurement by detectors, we first find out ideal probabilities along with actual probabilities for detection of photons in certain modes, then using Bayesian approach, we update our ideal conditional probabilities. In the following section we are going to naively discuss the teleportation scheme, which are very important to intuitively understand the concept of quantum teleportation.

1.5 Quantum Teleportation

Quantum teleportation is the process of transmitting an unknown quantum state of a particle from one place to another with the help of previously shared entangled particle between the sending and receiving locations and classical communication. Since teleportation depends on classical communication therefore it cannot be used to transport classical bits faster than light. It also obeys the no-cloning theorem, means that quantum system whose state we want to teleport do not traverse the distance between two location rather we destroy that particle by measuring it . Consider we have two parties Aalia and Babar separated in space. Aalia prepares an unknown qubit in quantum state $|\varphi\rangle = \alpha|0\rangle + \beta|1\rangle$ and wants to send it to Babar.We now explain quantum teleportation process, where we use one of the Bell states to carry out teleportation.

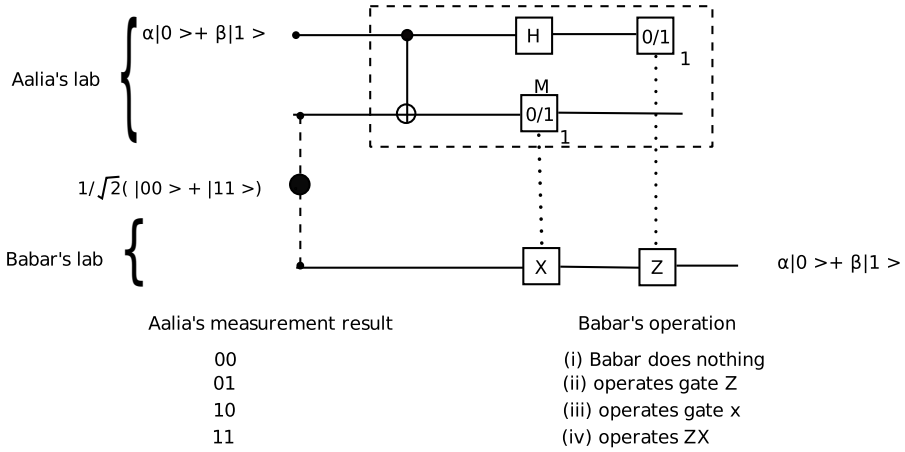

Figure 1.9: Quantum teleportation scheme, Bell state is used instead of stretched CNOT gate between both labs as a quantum channel.

1.5.1 Quantum Teleportation Using Bell State and Bell State Analyzer

In quantum teleportation scheme, the main challenge is to create quantum state $\alpha|00\rangle + \beta|11\rangle$ without using CNOT gate extending from Aalia to Babar's lab. In order to achieve this target we are going to discuss Bell states which are known to be maximally entangled two particle quantum states. These Bell states are given in Eqs. (1.27) - (1.30).

Assume that now Aalia and Babar share an entangled pair $|\phi^+\rangle$. Using this Bell state Aalia wants to teleport an unknown quantum state $\alpha|0\rangle + \beta|1\rangle$ from her lab to Babar's lab. First Aalia performs CNOT gate on her entangled qubit of pair and unknown qubit using later as control bit, so combined state will be

$$|\psi\rangle_{123} = (\alpha|0\rangle + \beta|1\rangle)_1(\frac{1}{\sqrt{2}}(|00\rangle + |11\rangle)_{23}) \quad = \quad \frac{\alpha}{\sqrt{2}}|000\rangle + \frac{\alpha}{\sqrt{2}}|011\rangle + \frac{\beta}{\sqrt{2}}|100\rangle + \frac{\beta}{\sqrt{2}}|111\rangle. \tag{1.56}$$

Apply CNOT on first two qubits of above equation using second qubit as target qubit

$$\begin{aligned} |\psi\rangle_{123} \quad \xrightarrow{CNOT_{12}} \quad & \frac{\alpha}{\sqrt{2}}|000\rangle + \frac{\alpha}{\sqrt{2}}|011\rangle + \frac{\beta}{\sqrt{2}}|110\rangle \\ & + \frac{\beta}{\sqrt{2}}|101\rangle = |\psi'\rangle_{123}. \end{aligned} \tag{1.57}$$

Combining first and third term and second with fourth term we have

$$|\psi^{'}\rangle_{123} = \frac{|0\rangle_2}{\sqrt{2}}(\alpha|00\rangle + \beta|11\rangle)_{13} + \frac{|1\rangle_2}{\sqrt{2}}(\alpha|01\rangle + \beta|10\rangle)_{13}. \tag{1.58}$$

Aalia performs measurement on her second qubit in $\{|0\rangle, |1\rangle\}$ basis. If Aalia's measurement results in state $|0\rangle$ then Aalia and Babar have remaining combine state $(\alpha|00\rangle+\beta|11\rangle)_{13}$ but in case if measurement outcome is state $|1\rangle$, then combined state will be $(\alpha|01\rangle + \beta|10\rangle)_{13}$.

So in first case of above measurements, Aalia and Babar achieve their target of getting state $(\alpha|00\rangle + \beta|11\rangle)_{13}$, but in second case they get combined state $(\alpha|01\rangle + \beta|10\rangle)_{13}$. Now Babar just performs flip operator to his qubit to get required target,

$$(\alpha|01\rangle + \beta|10\rangle)_{13} \xrightarrow{X_3} (\alpha|00\rangle + \beta|11\rangle)_{13}. \tag{1.59}$$

Aalia will perform Hadamard operator on her qubit and then measure it in $|0\rangle/|1\rangle$ basis.

$$\begin{aligned}(\alpha|00\rangle + \beta|11\rangle)_{13} \xrightarrow{H_1} & \frac{\alpha}{\sqrt{2}}|00\rangle + \frac{\alpha}{\sqrt{2}}|10\rangle + \frac{\beta}{\sqrt{2}}|01\rangle - \frac{\beta}{\sqrt{2}}|11\rangle \\ &= \frac{|0\rangle_1}{\sqrt{2}}(\alpha|0\rangle + \beta|1\rangle)_3 + \frac{|1\rangle_1}{\sqrt{2}}(\alpha|0\rangle - \beta|1\rangle)_3. \end{aligned} \tag{1.60}$$

If measurement on first qubit in basis $\{|0\rangle, |1\rangle\}$ after Hadamard operator results in state $|0\rangle$, then Babar's ends up with exactly the same qubit that Aalia wants to teleport, but if measurement results in state $|1\rangle$, Babar then applies phase operator to his qubit to get the teleported state. For summary see Fig. 1.9.

1.6 Thesis Outline

The thesis is organized as follows: In second chapter, we present the resources used for any quantum communication scheme, like quantum dense coding, entanglement swapping and quantum teleportation. Sections 2.1 to 2.3 represent the theory for entangled photons pair sources, then Sec. 2.4 briefly explain Bell state measurement and in Sec. 2.5 we show how to model different variety of photon detectors including ideal and actual photon detectors.

In the third chapter, we develop a model for practical quantum teleportation using the ingredients we developed in the second chapter. In Sec. 3.1 we explain teleportation

process in context of its origin. Section 3.2.1 and Sec. 3.2.2 covers Bell state measurement and projective measurement of photons in modes a and b, respectively. In Sec. 3.2.3 we find out probability of obtaining pure state at Babar mode. We then introduce the effect of detector inefficiencies on teleported state in Sec. 3.2.4. Finally Sec. 3.2.5 gives expression for fidelity in terms of detectors inefficiencies (η), dark counts probability (ρ_{dc}) and photon pair production rate.

Fourth chapter includes conclusion and graphs of fidelity versus photon pair generation rate χ, keeping dark count probability $\wp_{dc}$ constant and changing photon detectors efficiencies. Also we draw graphs of fidelity versus photon pair generation rate χ, keeping detectors efficiencies constant and changing dark count probabilities $\wp_{dc}$. Then we compared our theory with experimental paper and our simulated results are in good agreement with the experiment. We conclude in fifth chapter.

Chapter 2

Modeling Sources and Detectors

Different quantum communication processes such as quantum cryptography, quantum teleportation, quantum dense coding and linear optics quantum computing [3] use entangled photon pair sources. Most of these processes require bright, controlled and efficient sources of entanglement photon generation. Due to imperfect entangled photon pair sources and imperfect detectors, the theoretical realization of these processes involves extensive treatment of these resources . In this chapter; in Sec. 2.1 we describe experimental realization of entangled photon sources, then we explained mathematical formalism of practical sources in Sec. 2.2. In Sec. 2.3 we model resources for our practical quantum teleportation. Section 2.4 covers the detection of Bell states and finally in Sec. 2.5, we explained different kinds of detectors.

2.1 Spontaneous Parametric Down Conversion (SPDC)

The quantum correlation, entanglement, was first noticed between spatially separated quanta during measurement process of positron annihilation. Soon after Bohm's [14] proposal for observing EPR phenomenon in spin half systems and Bell's discovery that contradictory predictions between quantum theories can actually be observed, a series of experiments were performed, mostly using a polarization entangled photons from a two photon cascade emission from calcium . Using these techniques, it was noticed that the two photons were in the visible region, and could be controlled by using standard optical instruments. However the photons emitted are not in the opposite direction to conserve momentum, since the emitted atom carries away some randomly determined momentum. This makes it experimentally difficult to handle. On the other hand the process of parametric down conversion (PDC) can easily be handled and is more efficient

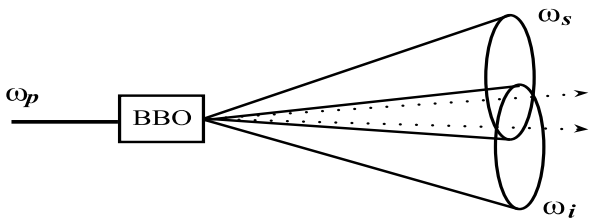

Figure 2.1: Spontaneous Parametric Down Conversion, a pump pulse with frequency ω_p after passing through nonlinear crystal like BBO, down converted into two entangled photons with frequencies ω_s and ω_i. The entangled photons lie, where both cones intersect each other given by dotted lines.

to produce entangled photon pair [15].

Spontaneous parametric down-conversion (also called SPDC, parametric scattering, or parametric fluorescence) is a fundamental process in quantum optics used as single photon source and entangle photons pair source. In this process photons from some source are bombarded on a nonlinear material which splits pump photon into two other photons satisfying the law of conservation of momentum and energy. The down converted photons are given names as signal and idler respectively. Now suppose that pump photon has frequency ω_p and momentum k_p, which after passing through nonlinear crystal e.g Beta-Barium Oxide (BBO) converted into two photons as signal with ω_s and momentum k_s and idler ω_i and momentum k_i, then according to the law of conservation of energy and momentum

$$\omega_p = \omega_s + \omega_i, \tag{2.1}$$
$$k_p = k_s + k_i, \tag{2.2}$$

as shown in Fig. 2.1. Photons from a pump laser beam down-converted in a nonlinear crystal, BBO, emerged pairwise, to the right, each in one of two cones, one as "signal" and other as "idler", with frequencies obeying phase-matching conditions corresponding to the conservation of momentum Note that this process is totally random, i.e., entangled pair of photons are produced randomly. When one photon (signal) is detected it guarantied that there must be its partner photon (idler). The SPDC is generally divided into two types, depending on the the polarization of entangled photon pair in our case (we will stick to the polarization property of photon through out our this study).

2.1.1 SPDC-TYPE-I

In SPDC TYPE-I, the pump laser beam converts into entangled photons having same polarization. Lets suppose that the incident pump laser has extraordinary polarization, then the entangled photons produced from this pulse after passing through the nonlinear medium have ordinary polarization. In perfect conditions such type of SPDC produces following Bell states.

$$|\phi^{\pm}\rangle = \frac{1}{\sqrt{2}}(|HH\rangle \pm |VV\rangle). \tag{2.3}$$

Using linear optics, it is impossible to detect which Bell state photons are between above two Bell states.

2.1.2 SPDC-TYPE-II

SPDC TYPE-II- results into entangled photons pair with different polarization, i.e., that both entangled photon have orthogonal polarization. Such type of effect is observed in materials with two different refractive indexes in two different directions such as calcite. If the pump laser beam has extraordinary polarization then after passing through such material like calcite it is down converted into two photons with ordinary and extra-ordinary polarization. SPDC TYPE-II with ideal conditions generally prepares the Bell states

$$|\psi^{\pm}\rangle = \frac{1}{\sqrt{2}}(|HV\rangle \pm |VH\rangle). \tag{2.4}$$

In reality the entangled state produced by these sources has less entanglement than Bell state.

2.2 Modeling Practical Sources

Quantum information (QI) processing and quantum communication are carried out by using practical sources. In this section we will model practical or imperfect sources which we can use in different QI process such as practical entanglement swapping, dense coding and especially in our case quantum teleportation. It is of great interest to have ideal entangled photon sources which on demand creates a single entangled-photons pair in Bell states, but such sources do not exist yet. On the other hand practical sources have probabilistic nature. Therefore such sources sometimes produces no entangled pair and the pump pulse goes without splitting and sometimes produces only one pair of entangled photons and some times produces more than one pair of entangled photons but all these

process are totally random and we do not know about specific phenomenon to happen at some particular time. In SPDC sources the rate of entangled photons generation is proportional to the nonlinearity $\chi^{(2)}$ of the material, the strength of pump laser and time of interaction of pump beam with material.

Lie Algebra SU(1,1) is used to describe SPDC transformation mathematically [16, 17]. Any set $\{N_x, N_y, N_z\}$ makes the basis of SU(1,1) algebra, if this set satisfies the following relations

$$[N_x, N_y] = -iN_z, \quad [N_y, N_z] = iN_x, \quad [N_z, N_x] = iN_y. \tag{2.5}$$

SU(1,1) realization for degenerate PDC or SPDC TYPE-I (i.e. two photons in entangled pair are identical) is a single mode realizations given by the generators

$$N_x^{(j)} = \frac{1}{4}(d_j^\dagger d_j^\dagger + d_j d_j), \tag{2.6}$$

$$N_y^{(j)} = \frac{1}{4i}(d_j^\dagger d_j^\dagger - d_j d_j), \tag{2.7}$$

$$N_z^{(j)} = \frac{1}{4}(d_j^\dagger d_j + d_j d_j^\dagger), \tag{2.8}$$

where, d_j refers to any of annihilation operators a_H, a_V, b_H and b_V.

On the other hand for SPDC TYPE-II or non-degenerate PDC, in which entangled photon are different, the appropriate SU(1,1) realizations are two mode realization given by the generators

$$N_x^{(ij)} = \frac{1}{2}(d_i^\dagger d_j^\dagger + d_i d_j), \tag{2.9}$$

$$N_y^{(ij)} = \frac{1}{2i}(d_i^\dagger d_j^\dagger - d_i d_j), \tag{2.10}$$

$$N_z^{(ij)} = \frac{1}{4}(d_i^\dagger d_j - d_i d_j^\dagger). \tag{2.11}$$

In SPDC TYPE-I both entangled photons have same polarization there for $d_i = a_H$ and $d_j = b_H$, where as in SPDC TYPE-II which creates entangled photons with different polarization thus we can use $d_i = a_H$ and $d_j = b_V$ in this situation. Finally SPDC process is mathematically represented and described by one parameter SU(1,1) transformation of the vacuum state as [18]

$$Z(\gamma) = \exp(i\gamma K_x)|\text{vac}\rangle, \quad \gamma \in R, \quad |\text{vac}\rangle = |0_H 0_V 0_H 0_V\rangle, \tag{2.12}$$

with K_x, one of generator from $\{K_x, K_y, K_z\}$ of SU(1,1) group satisfying following conditions

$$[K_x, K_y] = -iK_z, \quad [K_y, K_z] = iK_x, \quad [K_z, K_x] = iK_y. \tag{2.13}$$

Suppose the case of SPDC TYPE-I in which entangle photons pair have same polarization, the generator for such PDC is

$$K_x = \frac{1}{2}(a_H^\dagger b_H^\dagger + a_H b_H), \tag{2.14}$$

where a_H, b_H and $a_H^\dagger$, $b_H^\dagger$ are annihilation and creation operators corresponding to horizontal polarization of some spatial mode 'a' and 'b' respectively.

The resultant quantum state generated by practical source is not just a pair of photons but is in superposition of number states. It includes vacuum and pairs of pairs and even higher order terms. For some small value of 'γ', Eq. (2.12) can be written as

$$Z(\gamma) = |\text{vac}\rangle + \frac{i\gamma}{2}|1010\rangle, \qquad \gamma \in R \tag{2.15}$$

where, the Fock notation $|\text{ijkl}\rangle$ of the state represents a state with i, j, k, and l photons in a_H, a_V, b_H and b_V modes respectively with chosen order (HVHV). In Eq. (2.15), the vacuum part suggest that with high probability pump pulse will not convert into entangled photons.

2.3 Modeling of Practical Sources for Practical Quantum Teleportation

In our theory of quantum teleportation we need only one SPDC TYPE-II source. Such sources emits polarization entangled photons in some spatial modes, which are labeled as 'b' and 'c' . These photons have orthogonal polarization labeled as horizontal (H) and vertical (V). Basically we want to find out state generated by SPDC TYPE-II, which is similar to the following Bell state,

$$\begin{aligned} |\psi^-\rangle_{bc} &= \frac{1}{\sqrt{2}}(|HV\rangle - |VH\rangle)_{bc}, \\ &= \frac{1}{\sqrt{2}}(|1001\rangle - |0110\rangle)_{b_H b_V c_H c_V}. \end{aligned} \tag{2.16}$$

To create quantum state of the form $|\psi^-\rangle$, we use following generator of SU(1,1) group [18] in modes 'b' and 'c'

$$K_x = \frac{1}{2}(b_H^\dagger c_V^\dagger - b_V^\dagger c_H^\dagger + b_H c_V - b_V c_H), \tag{2.17}$$

$$K_y = \frac{1}{2i}(b_H^\dagger c_V^\dagger - b_V^\dagger c_H^\dagger - b_H c_V + b_V c_H), \tag{2.18}$$

$$K_z = \frac{1}{2}(b_H^\dagger b_H + c_V c_V^\dagger + b_V^\dagger b_V + c_H c_H^\dagger), \tag{2.19}$$

such that $\{K_x,\ K_y,\ K_z\}$ satisfies the conditions of SU(1,1) algebra given in Eq. (2.5). Therefore complete quantum state preprepared by such PDC is given as

$$|\chi\rangle \quad = \quad \exp[i\chi(b_H^\dagger c_V^\dagger - b_V^\dagger c_H^\dagger + b_H c_V - b_V c_H)]|\text{vac}\rangle, \tag{2.20}$$

where, parameter χ is considered as the efficiency of the source, such that $\chi = \frac{\gamma}{2} \in R$. As we know that

$$[a_i, a_j^\dagger] = \delta_{ij}, \quad [b_i, b_j^\dagger] = \delta_{ij}, \tag{2.21}$$

$$[a_i, b_j^\dagger] = 0, \quad [b_i, a_j^\dagger] = 0, \tag{2.22}$$

where, $i, j \in \{H, V\}$. Using above commutation relations in Eq. (2.20), we get after simplification

$$|\chi\rangle \quad = \quad \exp[i\chi(b_H^\dagger c_V^\dagger + b_H c_V)] \exp[-i\chi(b_V^\dagger c_H^\dagger + b_V c_H)]|\text{vac}\rangle, \tag{2.23}$$

as we know that above equation is not in normal order form in which creation operators lies on left side from annihilation operators and we know that working with normal order form is much easier, therefore Eq. (2.23) is rewritten in normal order form by selecting generators for SU(1,1) algebra as

$$J_+ = b^\dagger c^\dagger, \quad J_- = bc, \quad J_\circ = \frac{1}{2}(b^\dagger b + c^\dagger c + 1). \tag{2.24}$$

where $\{J_\circ, J_+, J_-\}$ are new generators of SU(1,1) algebra satisfying the following conditions

$$[J_-, J_+] = 2J_\circ, \quad [J_\circ, J_\mp] = \mp J_\mp. \tag{2.25}$$

The normal order form for such generators is [19]

$$\exp[\alpha_+ J_+ + \alpha_\circ J_\circ + \alpha_- J_-] = \exp[B_+ J_+] \exp[\ln(B_\circ) J_\circ] \exp[B_- J_-], \tag{2.26}$$

where $B_\mp, B_\circ$ are given as

$$\begin{aligned} B_\mp &= \frac{(\alpha_\mp/\vartheta)\sinh\vartheta}{\cosh\vartheta - (\frac{\alpha_\circ}{2\vartheta})\sinh\vartheta}, \\ B_\circ &= [\cosh\vartheta - (\frac{\alpha_\circ}{2\vartheta})\sinh\vartheta]^{-1}, \\ \vartheta &= [(\frac{\alpha_\circ}{2})^2 - \alpha_+\alpha_-]^{\frac{1}{2}}. \end{aligned} \tag{2.27}$$

Using Eq. (2.26), the normal order decomposition transformation, we can write

$$\begin{aligned}\exp[i\chi(b_H^\dagger c_V^\dagger + b_H c_V)] &= \exp[i\chi b_H^\dagger c_V^\dagger + i\chi b_H c_V] \\ &= \exp[\phi(\chi) b_H^\dagger c_V^\dagger]\exp[\omega(\chi)(b_H^\dagger b_H + c_V^\dagger c_V + 1)]\exp[\phi(\chi) b_H c_V],\end{aligned} \tag{2.28}$$

in this case $\alpha_+ = \alpha_- = i\chi$ and $\alpha_\circ = 0$, therefore using Eq. (2.27), we calculate values of $\phi(\chi)$ and $\omega(\chi)$ as follows

$$\phi(\chi) := i\tanh(\chi), \quad \omega(\chi) := -\ln[\cosh(\chi), \quad \vartheta = \chi. \tag{2.29}$$

Following the same method used for (2.28), we can write

$$\begin{aligned}\exp[-i\chi(b_V^\dagger c_H^\dagger + b_V c_H)] &= \exp[-i\chi b_V^\dagger c_H^\dagger - i\chi b_V c_H] \\ &= \exp[\phi^{'}(\chi) b_V^\dagger c_H^\dagger]\exp[\omega^{'}(\chi)(b_V^\dagger b_V + c_H^\dagger c_H + 1)]\exp[\phi^{'}(\chi) b_V c_H],\end{aligned} \tag{2.30}$$

with parameters

$$\phi^{'}(\chi) := -i\tanh(\chi), \quad \omega^{'}(\chi) := -\ln[\cosh(\chi), \quad \vartheta^{'} = \chi. \tag{2.31}$$

Comparing Eqs. (2.29) and (2.31), we concluded that

$$\phi^{'}(\chi) = -\phi(\chi), \quad \omega^{'}(\chi) = \omega(\chi), \text{and} \quad \vartheta^{'} = \vartheta. \tag{2.32}$$

Using above conditions, Eq. (2.30) can be written in following form

$$\exp[-i\chi(b_V^\dagger c_H^\dagger + b_V c_H)] = \exp[-\phi(\chi) b_V^\dagger c_H^\dagger]\exp[\omega(\chi)(b_V^\dagger b_V + c_H^\dagger c_H + 1)]\exp[\phi(\chi) b_V c_H]. \tag{2.33}$$

To obtain normal order form of quantum state produced by PDC source, we simply put Eqs. (2.28) and (2.33) into Eq. (2.23) and after rearranging terms, we get

$$\begin{aligned}|\chi\rangle &= \exp[\phi(\chi)(b_H^\dagger c_V^\dagger - b_V^\dagger c_H^\dagger)]\exp[\omega(\chi)(b_H^\dagger b_H + b_V^\dagger b_V + c_H^\dagger c_H + c_V^\dagger c_V + 2)] \\ &\quad \times \exp[\phi(\chi)(b_H c_V - b_V c_H)]|\text{vac}\rangle.\end{aligned} \tag{2.34}$$

Note that $|\text{vac}\rangle = |0_{b_H} 0_{b_V} 0_{c_H} 0_{c_V}\rangle$. Now looking at the above equation, it is straight forward that the last two exponential terms leave the vacuum state unchanged and thus simplifies to

$$|\chi\rangle = \exp[2\omega(\chi)]\exp[\phi(\chi)(b_H^\dagger c_V^\dagger - b_V^\dagger c_H^\dagger)]|\text{vac}\rangle. \tag{2.35}$$

In our theory of quantum teleportation we used Eq. (2.35), the normal order form of quantum state produced by SPDC TYPE-II source.

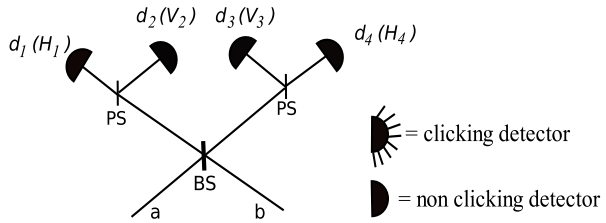

Figure 2.2: Bell state measurement setup, $d_i(H_i)$ for $i \in$ *(1,2,3,4)*, means i^{th} detector which can detect horizontal photon in i^{th} mode and beam splitter, polarization beam splitters are shown by BS, PBS respectively. The clicking detector shows that photon has been detected in certain mode by that detector.

2.4 Bell State Measurement

Generally QI can be encoded onto a quantum system by selecting the quantum state in which it is prepared. This information resides within the quantum system as long as system does not interact with the environment and we can retrieve this information whenever we want. The information retrieving is achieved by making measurements on the quantum system. In between preparation of quantum system and measurement, the information in quantum state, evolves in a manner determined by the Hamiltonian of the system. So in short measurement is a process through which we get information about any quantum system. In this section we will discuss how to measure Bell states.

Bell states are maximally entangled two particle quantum states, which are the main ingredient of many QI processes such as entanglement swapping [19], long distance quantum key distribution protocols [20], quantum dense coding [2], and in our case quantum teleportation [3]. Bell state measurement gives us two classical bits. It is observed that the interference of entangled particle in Bells state and the photon statistic behind the beam splitter shows in which Bell state the pair was [15].

Bell state measurement setup based on linear optics consists of a 50:50 beam splitter (BS), two polarization beam splitters (PBS) and four detectors as shown in the Fig. 2.2. It should be noted that clicking detectors shows that photons are detected in those modes.

In this setup we have two spatial modes 'a' and 'b' having polarized photons, incident on a 50:50 beam splitter (BS), which unitarily evolves these modes, and then interact with polarization beam splitter (PBS), which transmits horizontal polarized and reflects vertical polarized photons. Finally these photons are detected with the spatially separated detectors. Thus different polarization modes are detected by simple photo detectors in different spatial modes of photons. The clicking detectors shows that some photons are

detected in that specific mode where non clicking detector shows no photon detected. First we write Bell states in our representation

$$|\psi^{\pm}\rangle_{ab} = \frac{1}{\sqrt{2}}(|1001\rangle \pm |0110\rangle)_{a_H a_V b_H b_V}, \tag{2.36}$$

$$|\Phi^{\pm}\rangle_{ab} = \frac{1}{\sqrt{2}}(|1010\rangle \pm |0101\rangle)_{a_H a_V b_H b_V}, \tag{2.37}$$

$$|\psi^{\pm}\rangle_{ab} = \frac{1}{\sqrt{2}}(a^{\dagger}_{H_a} b^{\dagger}_{V_b}|0000\rangle \pm a^{\dagger}_{V_a} b^{\dagger}_{H_b}|0000\rangle), \tag{2.38}$$

$$|\Phi^{\pm}\rangle_{ab} = \frac{1}{\sqrt{2}}(a^{\dagger}_{H_a} b^{\dagger}_{H_b}|0000\rangle \pm a^{\dagger}_{V_a} b^{\dagger}_{V_b}|0000\rangle). \tag{2.39}$$

Now any modes either 'a' or 'b' with horizontal or vertical polarized photon when passes through the beam splitter (BS), changes according to following beam splitter transformations

$$a^{\dagger}_H \xrightarrow{U_{\rm BS}} \frac{1}{\sqrt{2}}(a^{\dagger}_{H_1} + ib^{\dagger}_{H_4}), \quad a^{\dagger}_V \xrightarrow{U_{\rm BS}} \tfrac{1}{\sqrt{2}}(a^{\dagger}_{V_2} + ib^{\dagger}_{V_3}), \tag{2.40}$$

$$b^{\dagger}_H \xrightarrow{U_{\rm BS}} \frac{1}{\sqrt{2}}(ia^{\dagger}_{H_1} + b^{\dagger}_{H_4}), \quad b^{\dagger}_V \xrightarrow{U_{\rm BS}} \tfrac{1}{\sqrt{2}}(ia^{\dagger}_{V_2} + b^{\dagger}_{V_3}). \tag{2.41}$$

Applying these transformation to Eqs. (2.38) and (2.39)

$$\begin{aligned} |\psi^{-}\rangle_{ab} \xrightarrow{U_{\rm BS}} & \frac{1}{\sqrt{2}}(\frac{1}{\sqrt{2}}(a^{\dagger}_{H_1} + ib^{\dagger}_{H_4}).\frac{1}{\sqrt{2}}(ia^{\dagger}_{V_2} + b^{\dagger}_{V_3})|0000\rangle \\ & -\frac{1}{\sqrt{2}}(a^{\dagger}_{V_2} + ib^{\dagger}_{V_3}).\frac{1}{\sqrt{2}}(ia^{\dagger}_{H_1} + b^{\dagger}_{H_4})|0000\rangle), \end{aligned}$$

$$\begin{aligned} |\psi^{-}\rangle_{ab} = & \frac{1}{2\sqrt{2}}((ia^{\dagger}_{H_1}a^{\dagger}_{V_2} - b^{\dagger}_{H_4}a^{\dagger}_{V_2} + a^{\dagger}_{H_1}b^{\dagger}_{V_3} + ib^{\dagger}_{H_4}b^{\dagger}_{V_3}) \\ & -(ia^{\dagger}_{V_2}a^{\dagger}_{H_1} - b^{\dagger}_{V_3}a^{\dagger}_{H_1} + a^{\dagger}_{V_2}b^{\dagger}_{H_4} + ib^{\dagger}_{V_3}b^{\dagger}_{H_4}))|0000\rangle, \end{aligned}$$

$$\begin{aligned} |\psi^{-}\rangle_{ab} &= \frac{1}{2\sqrt{2}}((i|1100\rangle - |0110\rangle + |1001\rangle + i|0011\rangle \\ &\quad -i|1100\rangle + |1001\rangle - |0110\rangle - i|0011\rangle)_{H_1V_2H_4V_3}, \\ &= \frac{1}{2\sqrt{2}}(2|1001\rangle - 2|0110\rangle)_{H_1V_2H_4V_3}, \\ |\psi^{-}\rangle_{ab} &= \frac{1}{\sqrt{2}}(|1001\rangle - |0110\rangle)_{H_1V_2H_4V_3}. \end{aligned} \tag{2.42}$$

Similarly we transform other Bell state in the same manner

$$\begin{aligned}|\psi^+\rangle_{ab} \xrightarrow{U_{\rm BS}} & \frac{1}{\sqrt{2}}(\frac{1}{\sqrt{2}}(a^\dagger_{H_1}+ib^\dagger_{H_4}).\frac{1}{\sqrt{2}}(ia^\dagger_{V_2}+b^\dagger_{V_3})|0000\rangle \\ & +\frac{1}{\sqrt{2}}(a^\dagger_{V_2}+ib^\dagger_{V_3}).\frac{1}{\sqrt{2}}(ia^\dagger_{H_1}+b^\dagger_{H_4})|0000\rangle),\end{aligned}$$

$$\begin{aligned}|\psi^+\rangle_{ab} &= \frac{1}{2\sqrt{2}}((ia^\dagger_{H_1}a^\dagger_{V_2}-b^\dagger_{H_4}a^\dagger_{V_2}+a^\dagger_{H_1}b^\dagger_{V_3}+ib^\dagger_{H_4}b^\dagger_{V_3}) \\ &\quad +(ia^\dagger_{V_2}a^\dagger_{H_1}-b^\dagger_{V_3}a^\dagger_{H_1}+a^\dagger_{V_2}b^\dagger_{H_4}+ib^\dagger_{V_3}b^\dagger_{H_4}))|0000\rangle,\end{aligned}$$

$$\begin{aligned}|\psi^+\rangle_{ab} &= \frac{1}{2\sqrt{2}}((i|1100\rangle-|0110\rangle+|1001\rangle+i|0011\rangle \\ &\quad +i|1100\rangle-|1001\rangle+|0110\rangle+i|0011\rangle)_{H_1V_2H_4V_3}, \\ |\psi^+\rangle_{ab} &= \frac{i}{\sqrt{2}}(|1100\rangle+|0011\rangle)_{H_1V_2H_4V_3}. \end{aligned} \tag{2.43}$$

Now for $|\Phi^+\rangle_{ab}$, we have

$$\begin{aligned}|\Phi^+\rangle_{ab} \xrightarrow{U_{\rm BS}} & \frac{1}{\sqrt{2}}(\frac{1}{\sqrt{2}}(a^\dagger_{H_1}+ib^\dagger_{H_4}).\frac{1}{\sqrt{2}}(ia^\dagger_{H_1}+b^\dagger_{H_4})|0000\rangle \\ & +\frac{1}{\sqrt{2}}(a^\dagger_{V_2}+ib^\dagger_{V_3}).\frac{1}{\sqrt{2}}(ia^\dagger_{V_2}+b^\dagger_{V_3})|0000\rangle), \\ = & \frac{1}{2\sqrt{2}}[(ia^\dagger_{H_1}a^\dagger_{H_1}+ib^\dagger_{H_4}b^\dagger_{H_4}+a^\dagger_{H_1}b^\dagger_{H_4}-a^\dagger_{H_1}b^\dagger_{H_4}) \\ & +(ia^\dagger_{V_2}a^\dagger_{V_2}+ib^\dagger_{V_3}b^\dagger_{V_3}+a^\dagger_{V_2}b^\dagger_{V_3}-a^\dagger_{V_2}b^\dagger_{V_3})]|0000\rangle,\end{aligned}$$

$$|\Phi^+\rangle = \frac{1}{2\sqrt{2}}[(ia^\dagger_{H_1}a^\dagger_{H_1}+ib^\dagger_{H_4}b^\dagger_{H_4})|0000\rangle+(ia^\dagger_{V_2}a^\dagger_{V_2}+ib^\dagger_{V_3}b^\dagger_{V_3})|0000\rangle],$$

$$|\Phi^+\rangle = \frac{i}{2\sqrt{2}}(\sqrt{2}|2000\rangle+\sqrt{2}|0020\rangle+\sqrt{2}|0200\rangle+\sqrt{2}|0002\rangle)_{H_1V_2H_4V_3},$$

$$|\Phi^+\rangle = \frac{i}{2}(|2000\rangle+|0200\rangle+|0020\rangle+|0002\rangle)_{H_1V_2H_4V_3}. \tag{2.44}$$

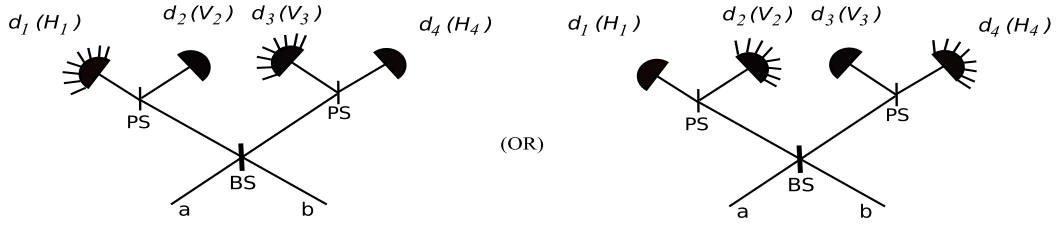

Figure 2.3: When detectors d_1 and d_3 **(OR)** d_2 and d_4 clicks, $|\psi^-\rangle$ state is detected.

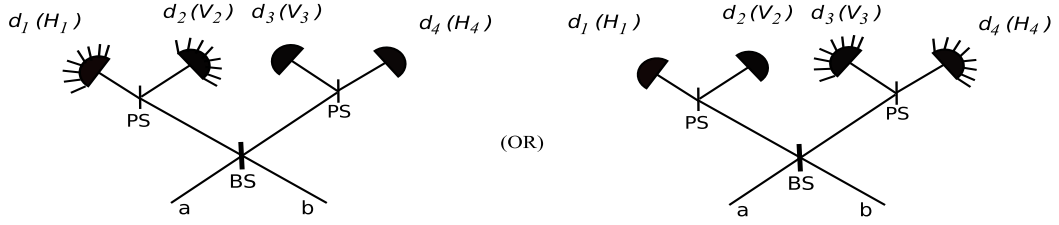

Figure 2.4: When detectors d_1 and d_2 **(OR)** d_3 and d_4 clicks, $|\psi^+\rangle$ state is detected, where symbols for clicking and non clicking detectors are given in Fig. 2.2.

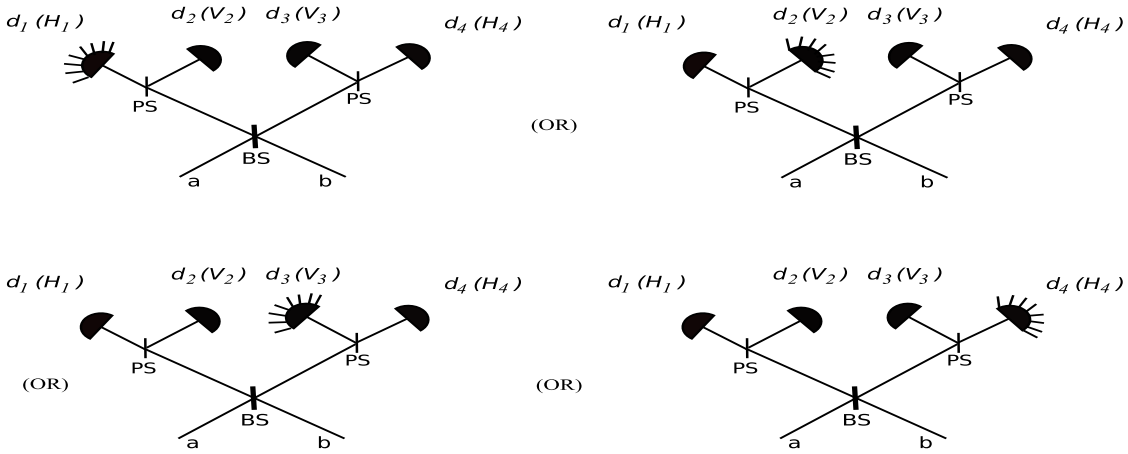

Figure 2.5: When detectors d_1 **(OR)** d_2 **(OR)** d_3 **(OR)** d_4 clicks, one of $|\Phi^{\pm}\rangle$ state is detected, it means to detect such type of Bell state only one of the four threshold detectors clicks, where symbols for clicking and non clicking detectors are given in Fig. 2.2.

Similarly after passing $|\Phi^-\rangle$ through beam splitter we get

$$|\Phi^-\rangle = \frac{i}{2}(|2000\rangle - |0200\rangle + |0020\rangle - |0002\rangle)_{H_1V_2H_4V_3}. \quad (2.45)$$

H_1, V_2, H_4, and V_3 represents the polarization of photons after beam splitter (BS) and polarization beam splitters (PBS) detected by detectors d_1, d_2, d_4, and d_3 respectively. So after passing through beam splitters and polarization beam splitters Bells states we got, are

$$|\psi^-\rangle = \frac{1}{\sqrt{2}}(|1001\rangle - |0110\rangle)_{H_1V_2H_4V_3}, \quad (2.46)$$

$$|\psi^+\rangle = \frac{i}{\sqrt{2}}(|1100\rangle + |0011\rangle)_{H_1V_2H_4V_3}, \quad (2.47)$$

$$|\Phi^\pm\rangle = \frac{i}{2}(|2000\rangle \pm |0200\rangle + |0020\rangle \pm |0002\rangle)_{H_1V_2H_4V_3}, \quad (2.48)$$

Eq. (2.46) shows that $|\psi^-\rangle$ is detected when detectors d_1 and d_3 or d_2 and d_4 clicks as shown in Fig. 2.3. On the other hand Eq. (2.47) shows that $|\psi^+\rangle$ is detected when detectors d_1 and d_2 or d_3 and d_4 click as depicted in Fig. 2.4. Equation (2.48) suggests that we cannot discriminate between $|\Phi^+\rangle$ and $|\Phi^-\rangle$ because in both these cases detector d_1 or d_2 or d_3 or d_4 detects two photons. Since we used threshold detectors, thus for both $|\Phi^\pm\rangle$ only one of the four detectors will clicks as shown in Fig. 2.5.

2.5 Detectors

Detectors are optical devices used in different QI process such as quantum teleportation, dense coding and entanglement swapping. In this section we discuss different kinds of detector model. Semiconductor based photon detector namely Indium-Gallium-Arsenide (InGaAs) avalanche photo-diodes detectors (APDs) [21], are able to detect single photons close to room temperature. These detectors use strong electric field within the semiconductor to accelerate electrons, and when a photon strikes the detectors an avalanche of electrons is generated, which triggers a click. There are some other detectors which have been prototyped. Superconducting transition-edge sensors (TES) are most notable of them, which are photon-number-resolving with detection efficiency up to 88 percent at 1550 nm and benefit from negligible dark count rates [20].

Generally detectors exhibit dark count which means that detector sometimes clicks even if there is no photon striking on it. So in reality it is still technological challenge to

invent ideal detectors. In following sections we are going to presents a brief theoretical description of imperfect detectors. To model such detectors we place a beam splitter in front of ideal detector which interfere the coherent input state with some thermal state representing dark counts and the other random errors.

2.5.1 Ideal Photon Number Discriminating Detectors

As clear from the name that such detectors always clicks when there are photons present in certain mode and never register a click when there are no photons. Information about the number of incident photons are provided by the strength of the click. Such detectors are mathematically represented by projective valued measurement (PVM)

$$\tilde{\prod}_i = |i\rangle\langle i|, \quad \text{where} \quad i = 0, 1, 2..... \tag{2.49}$$

in some fock basis state $|i\rangle, i \in N$ of certain mode. Now consider that we have more than one mode $|ijkl\rangle$ then the PVM for these modes will be of the form

$$\tilde{\prod}_{ijkl} = |i\rangle\langle i| \otimes |j\rangle\langle j| \otimes |k\rangle\langle k| \otimes |l\rangle\langle l|, \quad \text{where} \quad i, j, k, l = 0, 1, 2..... \tag{2.50}$$

2.5.2 Inefficient Photon Number Discriminating Detectors with no Dark Counts

In our theory, we represent the efficiency of detectors with η. Now inefficient photon number discriminating detectors are detectors having efficiency less than unity i.e., $0 < \eta < 1$, which means that there is finite probability that detector does not trigger a click if there are photons incident into the detector. To model such imperfect detectors, a beam splitter (BS) with transmittance η is placed in front of an ideal detector [22]. It should be noted that η is used for both transmittance and efficiency of detectors. Since in this case we have no dark counts which means that dark counts are zero. Therefore we take vacuum state together with photon signal state incident into the beam splitter as shown in the Fig. 2.6. Now the probability that such detectors measured 'q' photons when some signal with state ρ_{sig} incident into the detector is given as

$$p(q|\rho_{\text{sig}}) = Tr_{\text{tran}}[\tilde{\prod}_q Tr_{\text{ref}}\{U_{\text{BS}}(\eta)(\rho_{\text{sig}} \otimes |\text{vac}\rangle\langle\text{vac}|)U^{\dagger}_{\text{BS}}(\eta)\}\tilde{\prod}_q], \tag{2.51}$$

where $U_{\text{BS}}(\eta)$ represents the unitary transformation of beam splitter. Since we know that input signal state is in fock state such that $\rho_{\text{sig}} = |i\rangle\langle i|$, then conditional probability to detect 'q' photons with 'i' photons incident into the detector is

$$p(q|i) = Tr_{\text{tran}}[\tilde{\prod}_q Tr_{\text{ref}}\{U_{\text{BS}}(\eta)(|i\rangle\langle i| \otimes |\text{vac}\rangle\langle\ \text{vac}|)U^{\dagger}_{\text{BS}}(\eta)\}\tilde{\prod}_q], \tag{2.52}$$

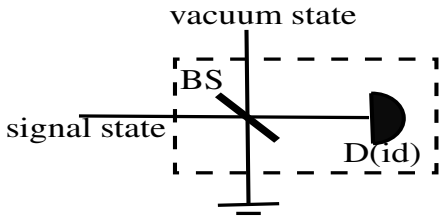

Figure 2.6: Inefficient Photon number Discriminating Detectors with no Dark Counts.

$$p(q|i) = \begin{cases} \begin{pmatrix} i \\ q \end{pmatrix} \eta^q (1-\eta)^{i-q} & \text{if i}\geq \text{ q} \\ 0 & \text{if i}< \text{ q}, \end{cases} \tag{2.53}$$

Eq. (2.53) shows that in order to detect 'q' photons, the number of incident photons 'i' must be greater than 'q', because in this model we do not include dark counts.

2.5.3 Inefficient Photon Number Discriminating Detectors with Dark Counts

In this model, together with detectors inefficiency 'η' , we take into account the dark counts possibility $\wp_{dc}$. Therefore we combine signal photons input state from one port of beam splitter with thermal state ρ_T [19] of the following form

$$\rho_T = \frac{1}{\cosh^2(r)} \sum_{n=0}^{\infty} \tanh^{2n}(r) |n\rangle\langle n|, \tag{2.54}$$

from the other input port of the beam splitter. These fictitious photons correspond to dark counts of the detector. Now we will find out conditional probability using such type of detector with efficiency η and dark count probability $\wp_{dc}$ as

$$p_{\eta,\wp_{dc}}(q|i) = Tr_{\text{tran}}[\tilde{\prod}_q Tr_{\text{ref}}\{U_{\text{BS}}(\eta)(|i\rangle\langle i| \otimes \rho_T|)U^{\dagger}_{\text{BS}}(\eta)\}\tilde{\prod}_q], \tag{2.55}$$

where $p_{\eta,\wp_{dc}}(q|i)$ is the probability of detecting 'q' photons in a mode given that 'i' photons are incident on the detector with efficiency η and dark counts probability $\wp_{dc}$. In this case due to dark counts probability, it is possible that the detected photons 'q' may be greater than 'i' . The dark counts probability $\wp_{dc}$ is given as [19]

$$\wp_{dc} = \frac{(1-\eta)\tanh^2 r}{1-\eta\tanh^2 r}. \tag{2.56}$$

Consider d, $d^\dagger$ (e, $e^\dagger$) are the annihilation and creation operators of signal (fictitious thermal) modes, respectively. Then the initial quantum state of both modes before beam splitter in the form of above operators will be

$$\begin{aligned}\rho^{\text{init}}_{\text{sig},T} = \rho_{\text{sig}} \otimes \rho_T &= \frac{1}{\cosh^2(r)} \sum_{n=0}^{\infty} \tanh^{2n}(r) |i,n\rangle\langle i,n|, \\ &= \frac{1}{\cosh^2(r)} \sum_{n=0}^{\infty} \frac{\tanh^{2n}(r)}{i!n!} d^{i\dagger} e^{n\dagger} |0,0\rangle\langle 0,0| d^i e^n. \end{aligned} \tag{2.57}$$

We pass above quantum state through a beam splitter with transformation matrix consisting of transmission coefficient $\sqrt{\eta}$ and reflection coefficient $\sqrt{1-\eta}$

$$U_{\text{BS}}(\eta) = \begin{pmatrix} \sqrt{\eta} & \sqrt{1-\eta} \\ -\sqrt{1-\eta} & \sqrt{\eta} \end{pmatrix}. \tag{2.58}$$

The operators $d, d^\dagger (e, e^\dagger)$ transformed by beam splitter as

$$\begin{pmatrix} d \\ e \end{pmatrix} \longrightarrow U^\dagger_{\text{BS}}(\eta) \begin{pmatrix} d \\ e \end{pmatrix}, \quad \begin{pmatrix} d^\dagger \\ e^\dagger \end{pmatrix} \longrightarrow U_{\text{BS}}(\eta) \begin{pmatrix} d^\dagger \\ e^\dagger \end{pmatrix}. \tag{2.59}$$

Thus after applying beam splitter transformation, $\rho^{\text{init}}_{\text{sig},T}$ changes to $\rho^{\text{out}}_{\text{sig},T}$ as

$$\rho^{\text{out}}_{\text{sig},T} = U_{\text{BS}}(\eta) \rho^{\text{init}}_{\text{sig},T} U^\dagger_{\text{BS}}(\eta), \tag{2.60}$$

$$\begin{aligned}\rho^{\text{out}}_{\text{sig},T} &= \frac{1}{\cosh^2(r)} \sum_{n=0}^{\infty} \frac{\tanh^{2n}(r)}{i!n!} (\sqrt{\eta} d^\dagger - \sqrt{1-\eta} e^\dagger)^i (\sqrt{1-\eta} d^\dagger + \sqrt{\eta} e^\dagger)^n \\ &\quad \times |0,0\rangle\langle 0,0| (\sqrt{\eta} d - \sqrt{1-\eta} e)^i (\sqrt{1-\eta} d + \sqrt{\eta} e)^n, \end{aligned} \tag{2.61}$$

$$\begin{aligned}\rho^{\text{out}}_{\text{sig},T} &= \frac{1}{\cosh^2(r)} \sum_{n=0}^{\infty} \frac{\tanh^{2n}(r)}{i!n!} \sum_{\lambda=0}^{i} \sum_{\lambda'=0}^{i} \sum_{\kappa=0}^{n} \sum_{\kappa'=0}^{n} \begin{pmatrix} i \\ \lambda \end{pmatrix} \begin{pmatrix} i \\ \lambda' \end{pmatrix} \begin{pmatrix} n \\ \kappa \end{pmatrix} \begin{pmatrix} n \\ \kappa' \end{pmatrix} (-1)^{\kappa+\kappa'} \\ &\quad (\sqrt{\eta})^{2n+\lambda+\lambda'-\kappa-\kappa'} (\sqrt{1-\eta})^{2i-\lambda-\lambda'+\kappa+\kappa'} (d^\dagger)^{\lambda+\kappa} (e^\dagger)^{i+n-\lambda-\kappa} |0,0\rangle \\ &\quad \otimes \langle 0,0| (d)^{\lambda'+\kappa'} (e)^{i+n-\lambda'-\kappa'}, \end{aligned} \tag{2.62}$$

$$\rho^{\text{out}}_{\text{sig},T} = \frac{1}{\cosh^2(r)} \sum_{n=0}^{\infty} \frac{\tanh^{2n}(r)}{i!n!} \sum_{\lambda=0}^{i} \sum_{\lambda'=0}^{i} \sum_{\kappa=0}^{n} \sum_{\kappa'=0}^{n} \binom{i}{\lambda} \binom{i}{\lambda'} \binom{n}{\kappa} \binom{n}{\kappa'} (-1)^{\kappa+\kappa'} (\sqrt{\eta})^{2n+\lambda+\lambda'-\kappa-\kappa'} (\sqrt{1-\eta})^{2i-\lambda-\lambda'+\kappa+\kappa'} \times |\lambda+\kappa, i+n-\lambda-\kappa\rangle\langle\lambda'+\kappa', i+n-\lambda'-\kappa'|. \quad (2.63)$$

To find out conditional probability Eq. (2.55) suggests that first trace out reflection mode, then project the remaining state on fock state $|q\rangle$ and finally trace out the transmitted mode of above equation

$$p_{\eta,\wp_{dc}}(q|i) = \frac{(1-\eta)^i}{\cosh^2 r} \left(\tfrac{\eta}{1-\eta} \right)^q \sum_{n=0}^{\infty} [\eta \tanh^2(r)]^n \left(\frac{q!(i+n-q)!}{i!n!}\right) [\Omega(i,q,\eta,n)]^2, \quad (2.64)$$

with

$$\Omega(i,q,\eta,n) := \sum_{\upsilon=0}^{n} \binom{i}{q-\upsilon} \binom{n}{\upsilon} \left(\tfrac{\eta-1}{\eta} \right)^{\upsilon}. \quad (2.65)$$

Since we know that number of detected photons by detector cannot be greater than sum of signal photon and thermal photons therefore $\Omega(i,q,\eta,n) = 0$ for $q > i+n$. Eq. (2.65) in factorial form can be written as following. First we take the case in which $q \geq i$

$$\Omega(i,q,\eta,n) := \sum_{\upsilon=0}^{n} \frac{i!n!}{(q-\upsilon)!(i-q+\upsilon)!\upsilon!(n-\upsilon)!} \left(\tfrac{\eta-1}{\eta} \right)^{\upsilon}. \quad (2.66)$$

To make above equation more compact, we introduce the concept of Hypergeometric function define as

$$F(\alpha,\beta,\gamma,x) = 1 + \sum_{i=1}^{\infty} \frac{(\alpha)_i (\beta)_i x^i}{i!(\gamma)_i}, \quad (2.67)$$

where $(z)_n$ is the Pochhammer symbol such that $(z)_n = \Gamma(z+n)/\Gamma(z)$ with Γ is the gamma function. Using properties of gamma functions we make q and n both negative, to get finite solution of Eq. (2.66)

$$\frac{q!}{(q-\upsilon)!} = \frac{\Gamma(q+1)}{\Gamma(q-\upsilon+1)} = \frac{\Gamma(-q+\upsilon)}{\Gamma(-q)} (-1)^{\upsilon}. \quad (2.68)$$

Similarly

$$\frac{n!}{(n-\upsilon)!} = \frac{\Gamma(n+1)}{\Gamma(n-\upsilon+1)} = \frac{\Gamma(-n+\upsilon)}{\Gamma(-n)}(-1)^{\upsilon}, \tag{2.69}$$

multiply and divide Eq. (2.66) by $q!(q-i)!$ we get

$$\Omega(i,q,\eta,n) := \sum_{\upsilon=0}^{n} \frac{i!q!n}{(q-\upsilon)!(q-i)!(i-q+\upsilon)(q-i)!\upsilon!(n-\upsilon)!} \left(\frac{\eta-1}{\eta} \right)^{\upsilon}. \tag{2.70}$$

Thus

$$\Omega(i,q,\eta,n) = \begin{pmatrix} i \\ q \end{pmatrix} \; {}_2F_1(-n,-q;i-q+1;\tfrac{\eta-1}{\eta}). \tag{2.71}$$

Now for $i < q$, we have

$$\Omega(i,q,\eta,n) = \sum_{\upsilon=0}^{n} \frac{i!n!}{(q-\upsilon)!(i-q+\upsilon)!\upsilon!(n-\upsilon)!} \left(\frac{\eta-1}{\eta} \right)^{\upsilon}. \tag{2.72}$$

putting $l = \upsilon - q + i$ in above equation.

$$\Omega(i,q,\eta,n) = \sum_{l=0}^{n-i+q} \frac{i!n!}{l!(i-l)!(l+q-i)!(n+i-q-l)!} \left(\frac{\eta-1}{\eta} \right)^{l+q-i}. \tag{2.73}$$

Multiply and divide above equation by $(n-q-i)!(q-i)!$, and then simplifying we get

$$\Omega(i,q,\eta,n) = \sum_{l=0}^{n-i+q} \left(\frac{\eta-1}{\eta} \right)^{q-i} \begin{pmatrix} n \\ q-i \end{pmatrix} \; {}_2F_1(-i,n-q+i;q-i+1;\tfrac{\eta-1}{\eta}). \tag{2.74}$$

Putting Eqs. (2.71) and (2.74) in Eq. (2.66) for finding conditional probability of detecting photons greater than or equal to incident signal photon and less than incident signal photon respectively with using following parameters

$$b(\eta,\wp_{dc}) := \eta \tanh^2 r = \frac{\eta\wp_{dc}}{1-\eta(1-\wp_{dc})}, \tag{2.75}$$

and

$$\frac{1}{\cosh^2 r} = \frac{(1-\eta)(1-\wp_{dc})}{1-\eta(1-\wp_{dc})}. \tag{2.76}$$

We get

$$p_{\eta,\wp_{dc}}(q|i) = \begin{cases} \frac{(1-\eta)(1-\wp_{dc})}{1-\eta(1-\wp_{dc})}(1-\eta)^i \left(\frac{\eta}{1-\eta} \right)^q \Omega(i,q,\eta,\wp_{dc}) & \text{if } i \geq q, \\ \frac{(1-\eta)(1-\wp_{dc})}{1-\eta(1-\wp_{dc})}\eta^i \left\{ \frac{1-\eta}{\eta} \; b(\eta,\wp_{dc}) \right\}^{q-i} \Omega(q,i,\eta,\wp_{dc}) & \text{if } i < q, \end{cases} \tag{2.77}$$

where

$$\begin{aligned} \Omega(x,y,\eta,\wp_{dc}) &= \sum_{n=0}^{\infty} \left(\begin{array}{c} x \\ y \end{array} \right) \left(\begin{array}{c} n+x-y \\ x-y \end{array} \right) (b(\eta,r))^n \\ &\quad \times \{ {}_2F_1(-n,-y;x-y+1,\frac{\eta-1}{\eta}) \}^2, \end{aligned} \tag{2.78}$$

and

$$\begin{aligned} \Omega(y,x,\eta,\wp_{dc}) &= \sum_{n=0}^{\infty} \left(\begin{array}{c} y \\ x \end{array} \right) \left(\begin{array}{c} n+y-x \\ y-x \end{array} \right) (b(\eta,r))^n \\ &\quad \times \{ {}_2F_1(-n,-x;y-x+1,\frac{\eta-1}{\eta}) \}^2. \end{aligned} \tag{2.79}$$

Equation (2.77), thus gives the probability of detecting 'q' photons such that 'i' photons are incident on inefficient photon number discriminating detector.

2.5.4 Threshold Detectors

Threshold detectors are easily available than photon number discriminating detectors. We have modeled threshold detectors in our Bell state measurement process. Ideal or unit efficiency threshold detectors with no dark counts are those which measure whether the incoming mode is vacuum state or has at least one photon. Mathematically ideal threshold detectors (ITD) are represented using following operators

$$\tilde{\prod}_{\circ} = |0\rangle\langle 0|, \quad \tilde{\prod}_{\circ}^{\perp} = \mathbb{I} - |0\rangle\langle 0|. \tag{2.80}$$

To realize practical threshold detector, we use same model as used in photon number discriminating detectors but replacing vacuum state with thermal state as shown in Fig. 2.7. To find out conditional probabilities we follow same method as we did for photon number discriminating detectors but in this case 'q' can take two values either click or no click corresponding to PVM's $\tilde{\prod}_{\circ}^{\perp}$ or $\tilde{\prod}_{\circ}$ respectively. In our case of Bell state measurement the signal mode state is given as $\rho_{\text{sig}} = |i\rangle\langle i|$. We now just put '$q = 0$' for no click in

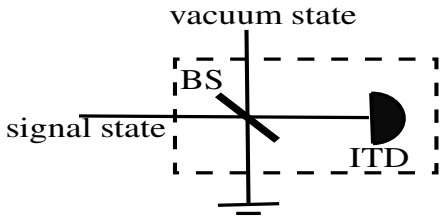

Figure 2.7: Threshold detector with efficiency η, signal and vacuum state of two different modes are incident on beam splitter with transmittance η, ITD represents ideal threshold detector.

Eq. (2.77) to get conditional probability for no-click. Where conditional probability for click is obtained by subtracting no-click probability from unity.

$$p_{\wp_{dc},\eta}(\text{no click}|i) = p_{\wp_{dc},\eta}(q=0|i) = (1-\wp_{dc})\{1-\eta(1-\wp_{dc})\}^i, \tag{2.81}$$

and thus the conditional probability of a click, when 'i' signal photons are incident is

$$p_{\wp_{dc},\eta}(\text{click}|i) \quad = 1 - p_{\wp_{dc},\eta}(\text{no click}|i) \quad = 1-(1-\wp_{dc})\{1-\eta(1-\wp_{dc})\}^i. \tag{2.82}$$

In our theory of teleportation, we used Eqs. (2.81) and (2.82), for no photon and some photons detection in Bell state measurement process.

We now develop model for quantum teleportation experiment using above mentioned practical resources in next chapter.

Chapter 3

Teleporting an Unknown Quantum State Using Practical Limitations

3.1 Introduction

Quantum teleportation is the process of sending quantum state of any physical quantum system from one place to another place without sending the original particle itself. Suppose we have sender and receiver named as Aalia and Babar respectively. Aalia wants to send an unknown polarization quantum state of a photon $\alpha|0\rangle + \beta|1\rangle$ to Babar's lab. One method is that Aalia measures her qubit and then send information to Babar through some classical channel. Since we know that measurement destroys the quantum state, therefore for Babar it will be impossible to get the exact replica of quantum state Aalia wants to teleport by using the measurement information sent by Aalia. In 1992 a group of six scientists [2] came up with a very fascinating idea that an unknown quantum state can be disassembled into purely classical information and quantum (EPR) correlations and then later reconstruct the same quantum state by using this information. To do so Aalia and Babar prearrange the sharing of entangled particle having Bell state. Aalia then performs a joint measurement (Bell state measurement) on the unknown quantum system and on her entangled particle of already shared entangled pair of particles. Knowing this classical information obtained by Aalia through Bell state measurement, Babar can convert the state of his particle of entangled pair into exact replica of the state Aalia wants to teleport by performing some unitary transformation on his qubit depending on the Bell state measurement performed by Aalia.

In 1997 quantum teleportation was for the first time, experimentally demonstrated with entangled photons [7]. Later, in laboratory different developments have been achieved in-

cluding open destination teleportation [24], entanglement swapping demonstration [25] and two-bit composite system teleportation [26]. In addition practical quantum teleportation through fiber link have been realized in [27, 28] and limited to one kilometer. Entangled photon pairs have been experimentally demonstrated over distance of 600m [29] and 13 km [30]. Later, over 144 km entangled photons were transmitted [31, 32]. Recently quantum teleportation over 16 km is demonstrated via free space links [33] using single entangled photons pair.

Teleportation is a kind of communication; it provides a way of of transporting a quantum state from one place to another, without having to move a physical system of that quantum state along with it. In our theory we used SPDC TYPE-II source to create entangled photons, laser pulses are pumped into BBO crystal which after passing through crystal convert into entangled photon pairs. Thus, in our calculations, we include multi-pair as well as vacuum state because to date no single pair photon pair producing sources exist. Actual sources used in the experiments are probabilistic which means that such sources randomly produce photon pairs in those instances in which laser pulse passes through the crystal.

This chapter is arranged as follows. Section 3.2.1 and Sec. 3.2.2 covers Bell state measurement and projective measurement of photons in modes a and b, respectively. In Sec. 3.2.3 we find out probability of obtaining pure state at Babar mode. We then introduce the effect of detector inefficiencies on teleported state in Sec. 3.2.4. Finally Sec. 3.2.5 gives expression for fidelity in terms of detectors inefficiencies (η), dark counts probability (ρ_{dc}) and photon pair production rate χ.

3.2 Practical Quantum Teleportation

Assume in our setup we have two parties, Aalia and Babar. Aalia wants to transmit an unknown quantum state to Babar. To do so, Aalia and Babar first need to share entangled photons. Therefore using practical PDC TYPE-II source, Aalia generate entanglement and sends one of entangled photons to Babar. Then passing her photon of entangled pair along with photon whose state is unknown, through Bell state analyzer. Bell state analyzer detects the entangled state of two photons. Beam splitter (BS) and polarization beam splitter (PBS) used in our practical model are perfect but photon detectors are faulty i.e., detector efficiency η, is less than one. We also include dark counts probability in our model. In pratical teleportation scheme, we have three spatial modes 'a', 'b' and 'c' . Photons in mode 'b' and 'c' are entangled. Modes 'a' and 'b' are then pass through BSM. Aalia then sends result of BSM to Babar through some classical channel. Babar apllies some unitary operator 'U' to his qubit depending upon results Aalia sent, as shown

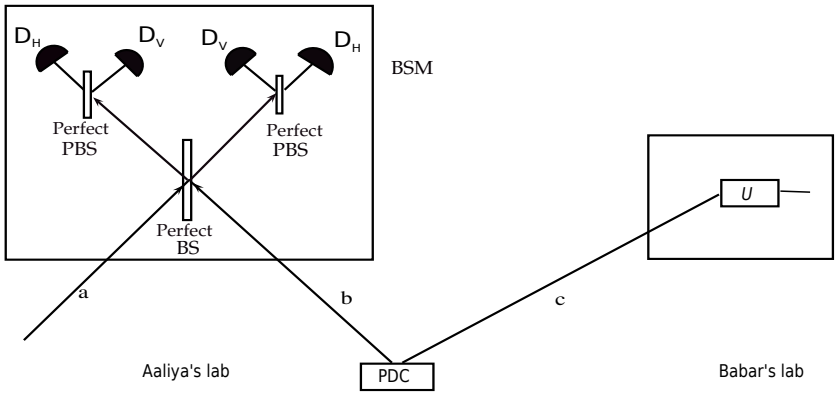

Figure 3.1: Practical quantum teleportation. BSM represents Bell state measurement setup. Where beam splitter and polarization beam splitter are shown by BS and PBS, respectively.

in Fig. 3.2. In folowing sections we explain practical teleportation in more detail.

3.2.1 Bell State Measurement

Aalia has PDC source which produces entangled photon pairs randomly. One photon from entangled pair in spatial mode 'b' is kept by Aalia and the second photon of pair in spatial mode 'c' is directed towards Babar. Quantum state prepared by single PDC-TYPE-II in normalized form given in Eq. (2.35) is

$$|\chi\rangle_{bc} = \exp[2\omega(\chi)] \exp[\phi(\chi)(b_H^\dagger c_V^\dagger - b_V^\dagger c_H^\dagger]|\text{vac}\rangle, \tag{3.1}$$

with $\omega(\chi) = -\ln[\cosh\chi]$ and $\phi(\chi) = i\tanh\chi$. Using Baker-Campbell-Hausdorff (BCH) formula

$$\exp(A+B) = \exp(A)\exp(B)\exp(-\frac{1}{2}[A,B]). \tag{3.2}$$

$$\exp[\phi(\chi)(b_H^\dagger c_V^\dagger - b_V^\dagger c_H^\dagger)] = \exp[\phi(\chi)(b_H^\dagger c_V^\dagger)]\exp[-\phi(\chi)(b_V^\dagger c_H^\dagger)], \tag{3.3}$$

therefore (3.1) can be written as

$$|\chi\rangle_{bc} = \exp[2\omega(\chi)] \exp[\phi(\chi)(b_H^\dagger c_V^\dagger)] \exp[-\phi(\chi)(b_V^\dagger c_H^\dagger)]|\text{vac}\rangle. \tag{3.4}$$

After Aalia has generated entangled photons using SPDC TYPE-II source, one photon of entangled pair is sent to the place where Aalia wants to teleport the unknown quantum state, for instance Babar's lab. The second partner of entangled pair and unknown quantum state of photon, is then subjected to Bell state measurement in Aalia's Lab. In our theory we take following unknown quantum state of photon that she wants to teleport

$$\begin{aligned} |\varphi\rangle_a = \alpha|H0\rangle + \beta|0V\rangle = \alpha|10\rangle + \beta|01\rangle, \\ |\varphi\rangle_a = \alpha a_H^\dagger|00\rangle + \beta a_V^\dagger|00\rangle, \\ |\varphi\rangle_a = \alpha a_H^\dagger|\text{vac}\rangle + \beta a_V^\dagger|\text{vac}\rangle. \end{aligned} \tag{3.5}$$

It is important to note that mode 'a' is used for unknown state to be teleported and 'b' and 'c' are used for entangled photons pair. Then the composite state $|\psi\rangle_{abc} = |\varphi\rangle_a \otimes |\chi\rangle_{bc}$ of above three photons is obtained by combining unknown quantum state in Eq. (3.5) and PDC state $|\chi\rangle$ of Eq. (3.4)

$$\begin{aligned} |\psi\rangle_{abc} = \alpha \exp[2\omega(\chi)] \exp[\phi(\chi)(b_H^\dagger c_V^\dagger)] \exp[-\phi(\chi)(b_V^\dagger c_H^\dagger)] a_H^\dagger|\text{vac}\rangle \\ +\beta \exp[2\omega(\chi)] \exp[\phi(\chi)(b_H^\dagger c_V^\dagger)] \exp[-\phi(\chi)(b_V^\dagger c_H^\dagger)] a_V^\dagger|\text{vac}\rangle, \end{aligned} \tag{3.6}$$

where $|\text{vac}\rangle = |000000\rangle = |HVHVHV\rangle$ or more generally
$|\text{vac}\rangle = |0_{a_H} 0_{a_V} 0_{b_H} 0_{b_V} 0_{c_H} 0_{c_V}\rangle$

To perform Bell state measurement Aalia first applies balanced beam splitter transformation to her modes 'a' and 'b' such that

$$a_H^\dagger \xrightarrow{U_{\text{BS}}} \frac{1}{\sqrt{2}}(a_H^\dagger - b_H^\dagger), \qquad b_H^\dagger \xrightarrow{U_{\text{BS}}} \frac{1}{\sqrt{2}}(a_H^\dagger + b_H^\dagger), \tag{3.7}$$

$$a_V^\dagger \xrightarrow{U_{\text{BS}}} \frac{1}{\sqrt{2}}(a_V^\dagger - b_V^\dagger), \qquad b_V^\dagger \xrightarrow{U_{\text{BS}}} \frac{1}{\sqrt{2}}(a_V^\dagger + b_V^\dagger). \tag{3.8}$$

It should be noted that photons in mode 'a' and 'b' are in the Aalia's lab. Above transformation on modes 'a' and 'b' which are initially in decomposable states yields

$$\begin{aligned} \boldsymbol{U}_{\text{BS}}^{ab}|\psi\rangle_{abc} &= \alpha \exp[2\omega(\chi)] \exp[\phi(\chi)(\frac{1}{\sqrt{2}}(a_H^\dagger + b_H^\dagger)c_V^\dagger)] \exp[-\phi(\chi)(\frac{1}{\sqrt{2}}(a_V^\dagger + b_V^\dagger)c_H^\dagger)] \\ &\times \frac{1}{\sqrt{2}}(a_H^\dagger - b_H^\dagger)|\text{vac}\rangle + \beta \exp[2\omega(\chi)] \exp[\phi(\chi)(\frac{1}{\sqrt{2}}(a_H^\dagger + b_H^\dagger)c_V^\dagger)] \\ &\times \exp[-\phi(\chi)(\frac{1}{\sqrt{2}}(a_V^\dagger + b_V^\dagger)c_H^\dagger)] \frac{1}{\sqrt{2}}(a_V^\dagger - b_V^\dagger)|\text{vac}\rangle. \end{aligned} \tag{3.9}$$

After further simplification using exponential expansion we get

$$\begin{aligned}\boldsymbol{U}_{\mathrm{BS}}^{ab}|\psi\rangle_{abc} &= \exp[2\omega(\chi)]\sum_{i'j'k'l'}(-1)^{k'+l'}\frac{[\phi(\chi)]^{i'+j'+k'+l'}c_H^{\dagger k'+l'}c_V^{\dagger i'+j'}}{\sqrt{2}^{i'+j'+k'+l'+1}i'!j'!k'!l'!}\\ &\times[\alpha(a_H^{\dagger i'+1}b_H^{\dagger j'}a_V^{\dagger k'}b_V^{\dagger l'}-a_H^{\dagger i'}b_H^{\dagger j'+1}a_V^{\dagger k'}b_V^{\dagger l'})\\ &+\beta(a_H^{\dagger i'}b_H^{\dagger j'}a_V^{\dagger k'+1}b_V^{\dagger l'}-a_H^{\dagger i'}b_H^{\dagger j'}a_V^{\dagger k'}b_V^{\dagger l'+1})]|\mathrm{vac}\rangle.\end{aligned}$$

Applying all creation operators of modes 'a' and 'b' on its vacuum state

$$\begin{aligned}\boldsymbol{U}_{\mathrm{BS}}^{ab}|\psi\rangle_{abc} &= \exp[2\omega(\chi)]\sum_{i'j'k'l'}(-1)^{k'+l'}\frac{[\phi(\chi)]^{i'+j'+k'+l'}c_H^{\dagger k'+l'}c_V^{\dagger i'+j'}}{\sqrt{2}^{i'+j'+k'+l'+1}i'!j'!k'!l'!}\\ &\times[\alpha(\sqrt{(i'+1)!j'!k'!l'!}|i'+1,k',j',l',00\rangle-\sqrt{i'!(j'+1)!k'!l'!}|i',k',j'+1,l',00\rangle)\\ &+\beta(\sqrt{i'!j'!(k'+1)!l'!}|i',k'+1,j',l',00\rangle-\sqrt{i'!j'!k'!(l'+1)!}|i',k',j',l'+1,00\rangle)].\end{aligned}$$

Finally we get

$$\begin{aligned}\boldsymbol{U}_{\mathrm{BS}}^{ab}|\psi\rangle_{abc} &= \exp[2\omega(\chi)]\sum_{i'j'k'l'}(-1)^{k'+l'}\frac{[\phi(\chi)]^{i'+j'+k'+l'}c_H^{\dagger k'+l'}c_V^{\dagger i'+j'}}{\sqrt{2}^{i'+j'+k'+l'+1}\sqrt{i'!j'!k'!l'!}}\\ &\times[\alpha(\sqrt{i'+1}|i'+1,k',j',l',00\rangle-\sqrt{j'+1}|i',k',j'+1,l',00\rangle)\\ &+\beta(\sqrt{k'+1}|i',k'+1,j',l',00\rangle-\sqrt{l'+1}|i',k',j',l'+1,00\rangle)].\end{aligned}\tag{3.10}$$

Equation (3.10) is the composite state of all three modes photons after passing modes 'a' and 'b' through a beam splitter (BS). In the following section we project this state on subspace.

3.2.2 Projective Measurement of two Particles at Sender

Now according to no-cloning theorem we cannot copy an unknown quantum state. In order to teleport state to Babar's lab, Aalia measures and hence destroys the quantum system which she wants to teleport, and hence does not violate no-cloning theorem. Aalia measures particle 'a' and 'b' in one of the four Bell states. This measurement projects

the total state in Eq.(3.10) to a subspace, where 'c' acquires the state of particle 'a'. This projective measurement is given as

$$\Pi^{ikjl}_{a_H a_V b_H b_V} = (|i\rangle\langle i|)_{a_H} \otimes (|k\rangle\langle k|)_{a_V} \otimes (|j\rangle\langle j|)_{b_H} \times (|l\rangle\langle l|)_{b_V} \otimes I_{c_H} \otimes I_{c_V}. \tag{3.11}$$

$$\begin{aligned}
\Pi^{ikjl}_{a_H a_V b_H b_V}(\boldsymbol{U}^{ab}_{\rm BS}|\psi\rangle_{abc}) &= \exp[2\omega(\chi)] \sum_{i'j'k'l'} (-1)^{k'+l'} \frac{[\phi(\chi)]^{i'+j'+k'+l'} c_H^{\dagger k'+l'} c_V^{\dagger i'+j'}}{\sqrt{2}^{i'+j'+k'+l'+1}\sqrt{i'!j'!k'!l'!}} \\
&\times[\alpha(\sqrt{i'+1}\delta_{i,i'+1}\delta_{k,k'}\delta_{j,j'}\delta_{l,l'} - \sqrt{j'+1}\delta_{i,i'}\delta_{k,k'}\delta_{j,j'+1}\delta_{l,l'}) \\
&+\beta(\sqrt{k'+1}\delta_{i,i'}\delta_{k,k'+1}\delta_{j,j'}\delta_{l,l'} - \sqrt{l'+1}\delta_{i,i'}\delta_{k,k'}\delta_{j,j'}\delta_{l,l'+1})] \\
&\times|i,k,j,l\rangle_{a_H,a_V,b_H,b_V} \otimes |00\rangle_{c_H,c_V}.
\end{aligned} \tag{3.12}$$

Now apply corresponding creation operators on the mode 'c' we have

$$\begin{aligned}
\Pi^{ikjl}_{a_H a_V b_H b_V}(\boldsymbol{U}^{ab}_{\rm BS}|\psi\rangle_{abc}) &= \exp[2\omega(\chi)] \sum_{i'j'k'l'} (-1)^{k'+l'} \frac{[\phi(\chi)]^{i'+j'+k'+l'}\sqrt{(k'+l')!(i'+j')!}}{\sqrt{2}^{i'+j'+k'+l'+1}\sqrt{i'!j'!k'!l'!}} \\
&\times[\alpha(\sqrt{i'+1}\delta_{i,i'+1}\delta_{k,k'}\delta_{j,j'}\delta_{l,l'} - \sqrt{j'+1}\delta_{i,i'}\delta_{k,k'}\delta_{j,j'+1}\delta_{l,l'}) \\
&+\beta(\sqrt{k'+1}\delta_{i,i'}\delta_{k,k'+1}\delta_{j,j'}\delta_{l,l'} - \sqrt{l'+1}\delta_{i,i'}\delta_{k,k'}\delta_{j,j'}\delta_{l,l'+1})] \\
&\times|i,k,j,l\rangle_{a_H,a_V,b_H,b_V} \otimes |k'+l', i'+j'\rangle_{c_H,c_V}.
\end{aligned}$$

$$
\begin{aligned}
\Pi^{ikjl}_{a_H a_V b_H b_V}(\boldsymbol{U}^{ab}_{\rm BS}|\psi\rangle_{abc}) \;=\; & \exp[2\omega(\chi)] \\
& \times[\alpha \sum_{i^{'}j^{'}k^{'}l^{'}} (-1)^{k^{'}+l^{'}} \frac{[\phi(\chi)]^{i^{'}+j^{'}+k^{'}+l^{'}} \sqrt{(k^{'}+l^{'})!(i^{'}+j^{'})!}}{\sqrt{2}^{i^{'}+j^{'}+k^{'}+l^{'}+1}\sqrt{i^{'}!j^{'}!k^{'}!l^{'}!}} \\
& \times\sqrt{i^{'}+1}\delta_{i,i^{'}+1}\delta_{k,k^{'}}\delta_{j,j^{'}}\delta_{l,l^{'}} \\
& -\alpha \sum_{i^{'}j^{'}k^{'}l^{'}} (-1)^{k^{'}+l^{'}} \frac{[\phi(\chi)]^{i^{'}+j^{'}+k^{'}+l^{'}} \sqrt{(k^{'}+l^{'})!(i^{'}+j^{'})!}}{\sqrt{2}^{i^{'}+j^{'}+k^{'}+l^{'}+1}\sqrt{i^{'}!j^{'}!k^{'}!l^{'}!}} \\
& \times\sqrt{j^{'}+1}\delta_{i,i^{'}}\delta_{k,k^{'}}\delta_{j,j^{'}+1}\delta_{l,l^{'}} \\
& +\beta \sum_{i^{'}j^{'}k^{'}l^{'}} (-1)^{k^{'}+l^{'}} \frac{[\phi(\chi)]^{i^{'}+j^{'}+k^{'}+l^{'}} \sqrt{(k^{'}+l^{'})!(i^{'}+j^{'})!}}{\sqrt{2}^{i^{'}+j^{'}+k^{'}+l^{'}+1}\sqrt{i^{'}!j^{'}!k^{'}!l^{'}!}} \\
& \times\sqrt{k^{'}+1}\delta_{i,i^{'}}\delta_{k,k^{'}+1}\delta_{j,j^{'}}\delta_{l,l^{'}} \\
& -\beta \sum_{i^{'}j^{'}k^{'}l^{'}} (-1)^{k^{'}+l^{'}} \frac{[\phi(\chi)]^{i^{'}+j^{'}+k^{'}+l^{'}} \sqrt{(k^{'}+l^{'})!(i^{'}+j^{'})!}}{\sqrt{2}^{i^{'}+j^{'}+k^{'}+l^{'}+1}\sqrt{i^{'}!j^{'}!k^{'}!l^{'}!}} \\
& \times\sqrt{l^{'}+1}\delta_{i,i^{'}}\delta_{k,k^{'}}\delta_{j,j^{'}}\delta_{l,l^{'}+1}] \\
& \times|i,k,j,l\rangle_{a_H,a_V,b_H,b_V} \otimes |k^{'}+l^{'},i^{'}+j^{'}\rangle_{c_H,c_V}.
\end{aligned}
$$

To get fruitfull equation by using property of Kronecker deltas, we must put $i^{'}=i-1$, $k^{'}=k$, $j^{'}=j$, $l^{'}=l$ in first 'α'term , $i^{'}=i$, $k^{'}=k$, $j^{'}=j-1$, $l^{'}=l$ in second 'α' term , $i^{'}=i$, $k^{'}=k-1$, $j^{'}=j$, $l^{'}=l$ in first 'β' term and $i^{'}=i$, $k^{'}=k$, $j^{'}=j$, $l^{'}=l-1$ in second 'β' term of Eq. (3.13).

$$\begin{aligned}\Pi^{ikjl}_{a_Ha_Vb_Hb_V}(\boldsymbol{U}^{ab}_{\rm BS}|\psi\rangle_{abc}) &= \exp[2\omega(\chi)][\alpha(-1)^{k+l}(\frac{[\phi(\chi)]^{i+j+k+l-1}\sqrt{(i+j-1)!(k+l)!}}{\sqrt{2}^{i+j+k+l}\sqrt{(i-1)!j!k!l!}}\sqrt{i}\\ &-\frac{[\phi(\chi)]^{i+j+k+l-1}\sqrt{(i+j-1)!(k+l)!}}{\sqrt{2}^{i+j+k+l}\sqrt{i!(j-1)!k!l!}}\sqrt{j})\\ &\times|ikjl\rangle_{a_H,a_V,b_H,b_V}\otimes|k+l,i+j-1\rangle_{c_H,c_V}\\ &+\beta(-1)^{k+l-1}(\frac{[\phi(\chi)]^{i+j+k+l-1}\sqrt{(i+j)!(k+l-1)!}}{\sqrt{2}^{i+j+k+l}\sqrt{i!j!(k-1)!l!}}\sqrt{k}\\ &-\frac{[\phi(\chi)]^{i+j+k+l-1}\sqrt{(i+j)!(k+l-1)!}}{\sqrt{2}^{i+j+k+l}\sqrt{i!j!k!(l-1)!}}\sqrt{l})\\ &\times|ikjl\rangle_{a_H,a_V,b_H,b_V}\otimes|k+l-1,i+j\rangle_{c_H,c_V}]. \qquad (3.13)\end{aligned}$$

Further simplification gives

$$\begin{aligned}\Pi^{ikjl}_{a_Ha_Vb_Hb_V}(\boldsymbol{U}^{ab}_{\rm BS}|\psi\rangle_{abc}) &= |ikjl\rangle_{a_H,a_V,b_H,b_V}\otimes\exp[2\omega(\chi)]\frac{(-1)^{k+l}[\phi(\chi)]^{i+j+k+l-1}}{\sqrt{2}^{i+j+k+l}}\\ &\times[\alpha\frac{\sqrt{(i+j-1)!(k+l)!}}{\sqrt{k!l!}}(\frac{\sqrt{i}}{\sqrt{(i-1)!j!}}-\frac{\sqrt{j}}{\sqrt{i!(j-1)!}})\\ &\times|k+l,i+j-1\rangle_{c_H,c_V}+\beta\frac{\sqrt{(i+j)!(k+l-1)!}}{\sqrt{i!j!}}\\ &\times(-\frac{\sqrt{k}}{\sqrt{(k-1)!l!}}+\frac{\sqrt{l}}{\sqrt{k!(l-1)!}})|k+l-1,i+j\rangle_{c_H,c_V}].\end{aligned}$$

Since $n!=n(n-1)!\Rightarrow(n-1)!=\frac{n!}{n}\Rightarrow\frac{1}{(n-1)!}=\frac{n}{n!}$. Using this identity in above equation.

$$\begin{aligned}\Pi^{ikjl}_{a_Ha_Vb_Hb_V}(\boldsymbol{U}^{ab}_{\rm BS}|\psi\rangle_{abc}) &= |ikjl\rangle_{a_H,a_V,b_H,b_V}\otimes\exp[2\omega(\chi)]\frac{(-1)^{k+l}[\phi(\chi)]^{i+j+k+l-1}}{\sqrt{2}^{i+j+k+l}\sqrt{i!j!k!l!}}\\ &\times[\alpha\sqrt{(i+j-1)!(k+l)!}(i-j)|k+l,i+j-1\rangle_{c_H,c_V}\\ &+\beta\sqrt{(i+j)!(k+l-1)!}(l-k)|k+l-1,i+j\rangle_{c_H,c_V}]. \qquad (3.14)\end{aligned}$$

Since we project our state onto subspace, which means that we measured photons in modes 'a' and 'b' and hence measurement destroys modes 'a' and 'b', therefore we discard

$|ikjl\rangle_{a_H,a_V,b_H,b_V}$ from Eq. (3.14), thus remaining state will be the state of Babar's photon which is in mode 'c' given below

$$\begin{aligned}\Pi^{ikjl}_{a_Ha_Vb_Hb_V}(\boldsymbol{U}^{ab}_{\rm BS}|\psi\rangle_{abc}) &= \exp[2\omega(\chi)]\frac{(-1)^{k+l}[\phi(\chi)]^{i+j+k+l-1}}{\sqrt{2}^{i+j+k+l}\sqrt{i!j!k!l!}}\\ &\times[\alpha\sqrt{(i+j-1)!(k+l)!}(i-j)|k+l,i+j-1\rangle_{c_H,c_V}\\ &+\beta\sqrt{(i+j)!(k+l-1)!}(l-k)|k+l-1,i+j\rangle_{c_H,c_V}].\end{aligned} \tag{3.15}$$

Since Eq. (3.15) is not normalized quantum state, therefore in Sec. 3.2.3 we normalize state at the Babar mode.

3.2.3 Probability of Obtaining Pure State at Receiver after Projective Measurement of Two Particles at Sender

We find the probability of resultant state at Babar after projecting the state to $ikjl$ photons in four modes at Aaliya's perfect detectors as $p(ikjl)$. This probability is given by normalizing quantum state in Eq. (3.15), such that

$$\langle\psi|(\Pi^{ikjl}_{a_Ha_Vb_Hb_V}\boldsymbol{U}^{ab}_{\rm BS})^\dagger\Pi^{ikjl}_{a_Ha_Vb_Hb_V}(\boldsymbol{U}^{ab}_{\rm BS}|\psi\rangle) = p(ikjl). \tag{3.16}$$

$$\begin{aligned}p(ikjl) &= \left(\exp[2\omega(\chi)]\frac{(-1)^{k+l}[\phi(\chi)]^{i+j+k+l-1}}{\sqrt{2}^{i+j+k+l}\sqrt{i!j!k!l!}}\right)^2\\ &\times\Big[(\alpha^*\sqrt{(i+j-1)!(k+l)!}(i-j)\langle k+l,i+j-1|\\ &+\beta^*\sqrt{(i+j)!(k+l-1)!}(l-k)\langle k+l-1,i+j|)\\ &\times(\alpha\sqrt{(i+j-1)!(k+l)!}(i-j)|k+l,i+j-1\rangle\\ &+\beta\sqrt{(i+j)!(k+l-1)!}(l-k)|k+l-1,i+j\rangle)\Big].\end{aligned}$$

After straight forward calculation

$$\begin{aligned}p(ikjl) &= \left(\exp[2\omega(\chi)]\frac{(-1)^{k+l}[\phi(\chi)]^{i+j+k+l-1}}{\sqrt{2}^{i+j+k+l}\sqrt{i!j!k!l!}}\right)^2\\ &\times[\alpha^2(i+j-1)!(k+l)!(i-j)^2+\beta^2(i+j)!(k+l-1)!(l-k)^2].\end{aligned}$$

$$\begin{aligned} p(ikjl) &= \exp[4\omega(\chi)]\frac{[\phi(\chi)]^{2(i+j+k+l-1)}}{2^{i+j+k+l}i!j!k!l!} \\ &\times[\alpha^2(i+j-1)!(k+l)!(i-j)^2+\beta^2(i+j)!(k+l-1)!(l-k)^2]. \end{aligned} \tag{3.17}$$

Putting values $\omega(\chi)$ and $\phi(\chi)$ in above equation we get

$$\begin{aligned} p(ikjl) &= \frac{[\tanh\chi]^{2(i+j+k+l-1)}}{\cosh^4\chi(2^{i+j+k+l}i!j!k!l!)} \\ &\times[\alpha^2(i+j-1)!(k+l)!(i-j)^2+\beta^2(i+j)!(k+l-1)!(k-l)^2]. \end{aligned} \tag{3.18}$$

Now first taking square root of (3.17) and then dividing (3.15) by it, we find the normalized state at Babar as

$$\begin{aligned} |\Phi\rangle_{c_H,c_V}^{ikjl} &= \frac{\Pi_{a_Ha_Vb_Hb_V}^{ikjl}(\boldsymbol{U}_{\mathrm{BS}}^{ab}|\psi\rangle_{abc})}{\sqrt{p(ikjl)}} \\ &= \frac{1}{[\alpha^2(i+j-1)!(k+l)!(i-j)^2+\beta^2(i+j)!(k+l-1)!(l-k)^2]^{\frac{1}{2}}} \\ &\times[\alpha\sqrt{(i+j-1)!(k+l)!}(i-j)|k+l,i+j-1\rangle_{c_H,c_V} \\ &+\beta\sqrt{(i+j)!(k+l-1)!}(l-k)|k+l-1,i+j\rangle_{c_H,c_V}], \end{aligned} \tag{3.19}$$

where $(ikjl)$ is readout of using ideal detectors.

3.2.4 Effect of Detector Inefficiencies on State at Receiver

Since we cannot have ideal detectors, therefore we use inefficient detectors and find actual readout $(qrst)$, then quantum state of the remaining mode is of the form

$$\varrho^{qrst} = \sum_{ijkl} P_{ikjl}^{qrst}|\Phi\rangle_{c_H,c_V}^{ikjl}\langle\Phi|, \tag{3.20}$$

with P_{ikjl}^{qrst}, using Bayesian inference in Eq. (1.46), we can write

$$\begin{aligned} P_{ikjl}^{qrst} &= P(ikjl|qrst) \\ &= \frac{p(qrst|ikjl)p(ikjl)}{p(qrst)} \\ P_{ikjl}^{qrst} &= \frac{p(qrst|ikjl)p(ikjl)}{\sum_{i_1j_1k_1l_1} p(qrst|i_1k_1j_1l_1)p(i_1k_1j_1l_1)}. \end{aligned} \tag{3.21}$$

As by Eq. (3.18)

$$\begin{aligned} p(ikjl) &= \frac{[\tanh\chi]^{2(i+j+k+l-1)}}{\cosh^4\chi(2^{i+j+k+l}i!j!k!l!)} \\ &\times[\alpha^2(i+j-1)!(k+l)!(i-j)^2+\beta^2(i+j)!(k+l-1)!(k-l)^2]. \end{aligned} \tag{3.22}$$

In order to find out $p(i_1k_1j_1l_1)$, we simply put $i=i_1$, $k=k_1$, $j=j_1$, $l=l_1$ in above equation.

Thus Eq. (3.21) after simplification leads us to the following equation.

$$\begin{aligned} P_{ikjl}^{qrst} &= \frac{p(qrst|ikjl)[\tanh\chi]^{2(i+j+k+l)}}{Z^{qrst}\times(2^{i+j+k+l}i!j!k!l!)} \\ &\times[\alpha^2(i+j-1)!(k+l)!(i-j)^2+\beta^2(i+j)!(k+l-1)!(l-k)^2], \end{aligned} \tag{3.23}$$

with

$$Z^{qrst} = \sum_{i_1j_1k_1l_1} \frac{p(qrst|i_1k_1j_1l_1)[\tanh\chi]^{2(i_1+k_1+j_1+l_1)}.E^{(i_1k_1j_1l_1)}}{2^{i_1+j_1+k_1+l_1}i_1!j_1!k_1!l_1!}, \tag{3.24}$$

where

$$E^{(i_1k_1j_1l_1)} = [\alpha^2(i_1+j_1-1)!(k_1+l_1)!(i_1-j_1)^2+\beta^2(i_1+j_1)!(k_1+l_1-1)!(l_1-k_1)^2]. \tag{3.25}$$

Now we find quantum fidelity of mixed state ϱ^{qrst} with respect to state $|\varphi\rangle$ in following section.

3.2.5 Fidelity of Final State at Receiver

We can find overlap of the actual state obtained at Babar with the state $|\varphi\rangle = \alpha|10\rangle+\beta|01\rangle$. This overlap is known as fidelity(F) with $0 \leq F \leq 1$. For $F = 0$, no overlap, where as for $F = 1$, the overlap is maximum. We use following formula

$$F^{qrst} = \sqrt{\langle\varphi|\varrho^{qrst}|\varphi\rangle}$$

$$F^{qrst} = \sqrt{\sum_{ijkl} P^{qrst}_{ikjl} \langle\varphi|\Phi\rangle^{ikjl}_{c_H,c_V} \langle\Phi|\varphi\rangle}. \tag{3.26}$$

Lets find out ($|\Phi\rangle^{ikjl}_{c_H,c_V}\langle\Phi|$) first.

For simplicity suppose ($|\Phi\rangle^{ikjl}_{c_H,c_V}\langle\Phi|$) = $|\Phi\rangle\langle\Phi|$. So we have to take outer product of Eq. (3.19) with it self

$$\begin{aligned}
|\Phi\rangle\langle\Phi| &= \frac{1}{(\alpha^2(i+j-1)!(k+l)!(i-j)^2+\beta^2(i+j)!(k+l-1)!(l-k)^2)} \\
&\times[\alpha^2(i+j-1)!(k+l)!(i-j)^2|k+l,i+j-1\rangle\langle k+l,i+j-1| \\
&+\beta^2(i+j)!(k+l-1)!(l-k)^2|k+l-1,i+j\rangle\langle k+l-1,i+j| \\
&+\alpha\beta\sqrt{(i+j)!(i+j-1)!(k+l)!(k+l-1)!}(i-j)(l-k) \\
&\times(|k+l,i+j-1\rangle\langle k+l-1,i+j|+|k+l-1,i+j\rangle\langle k+l,i+j-1|)].
\end{aligned} \tag{3.27}$$

Considering

$$\begin{aligned}
a &= \alpha^2(i+j-1)!(k+l)!(i-j)^2, && (3.28)\\
b &= \beta^2(i+j)!(k+l-1)!(l-k)^2, && (3.29)\\
c &= \alpha\beta\sqrt{(i+j)!(i+j-1)!(k+l)!(k+l-1)!}(i-j)(l-k), && (3.30)\\
d &= \alpha^2(i+j-1)!(k+l)!(i-j)^2+\beta^2(i+j)!(k+l-1)!(l-k)^2, && (3.31)\\
\Rightarrow d &= a+b. && (3.32)
\end{aligned}$$

Eq. (3.27) becomes

$$\begin{aligned}
|\Phi\rangle\langle\Phi| &= \frac{1}{d}[a|k+l,i+j-1\rangle\langle k+l,i+j-1|+b|k+l-1,i+j\rangle\langle k+l-1,i+j| \\
&+c(|k+l,i+j-1\rangle\langle k+l-1,i+j|+|k+l-1,i+j\rangle\langle k+l,i+j-1|)].
\end{aligned} \tag{3.33}$$

Next step is to find out expression for $\langle\varphi|\Phi\rangle_{c_H,c_V}\langle\Phi|\varphi\rangle = \langle\varphi|\Phi\rangle\langle\Phi|\varphi\rangle$

$$\begin{aligned}\langle\varphi|\Phi\rangle\langle\Phi|\varphi\rangle &= (\alpha^*\langle 10| + \beta^*\langle 01|)\\ &\times(\frac{1}{d}[a|k+l, i+j-1\rangle\langle k+l, i+j-1| + b|k+l-1, i+j\rangle\langle k+l-1, i+j|\\ &+c(|k+l, i+j-1\rangle\langle k+l-1, i+j| + |k+l-1, i+j\rangle\langle k+l, i+j-1|)])\\ &\times(\alpha|10\rangle + \beta|01\rangle). \end{aligned} \tag{3.34}$$

$$\begin{aligned}\langle\varphi|\Phi\rangle\langle\Phi|\varphi\rangle &= \frac{1}{d}[\underline{a\alpha^2\delta_{1,k+l}\delta_{0,i+j-1}\delta_{k+l,1}\delta_{i+j-1,0}} + \underline{b\alpha^2\delta_{1,k+l-1}\delta_{0,i+j}\delta_{k+l-1,1}\delta_{i+j,0}}\\ &+c\alpha^2\delta_{1,k+l}\delta_{0,i+j-1}\delta_{k+l-1,1}\delta_{i+j,0} + c\alpha^2\delta_{1,k+l-1}\delta_{0,i+j}\delta_{k+l,1}\delta_{i+j-1,0}\\ &+a\alpha\beta\delta_{1,k+l}\delta_{0,i+j-1}\delta_{k+l,0}\delta_{i+j-1,1} + b\alpha\beta\delta_{1,k+l-1}\delta_{0,i+j}\delta_{k+l-1,0}\delta_{i+j,1}\\ &+\underline{c\alpha\beta\delta_{1,k+l}\delta_{0,i+j-1}\delta_{k+l-1,0}\delta_{i+j,1}} + c\alpha\beta\delta_{1,k+l-1}\delta_{0,i+j}\delta_{k+l,0}\delta_{i+j-1,1}\\ &+a\alpha\beta\delta_{0,k+l}\delta_{1,i+j-1}\delta_{k+l,1}\delta_{i+j-1,0} + b\alpha\beta\delta_{0,k+l-1}\delta_{1,i+j}\delta_{k+l-1,1}\delta_{i+j,0}\\ &+c\alpha\beta\delta_{0,k+l}\delta_{1,i+j-1}\delta_{k+l-1,1}\delta_{i+j,0} + \underline{c\alpha\beta\delta_{0,k+l-1}\delta_{1,i+j}\delta_{k+l,1}\delta_{i+j-1,0}}\\ &+\underline{a\beta^2\delta_{0,k+l}\delta_{1,i+j-1}\delta_{k+l,0}\delta_{i+j-1,1}} + \underline{b\beta^2\delta_{0,k+l-1}\delta_{1,i+j}\delta_{k+l-1,0}\delta_{i+j,1}}\\ &+c\beta^2\delta_{0,k+l}\delta_{1,i+j-1}\delta_{k+l-1,0}\delta_{i+j,1} + c\beta^2\delta_{0,k+l-1}\delta_{1,i+j}\delta_{k+l,0}\delta_{i+j-1,1}]. \end{aligned} \tag{3.35}$$

Using property of Kronecker delta

$$\delta_{ij} = \begin{cases} 1 & \text{if } i = j \\ 0 & \text{otherwise,} \end{cases} \tag{3.36}$$

Consider Kronecker delta $\delta_{i,1}$, this means that only at i =1 it gives 1, otherwise delta gives zero i.e., for any value of 'i' except '1'. So if we have multiplication of two Kronecker deltas for instant $\delta_{i,1}\delta_{i,2}$, its multiplication always results into '0', because if Kronecker delta at i =1 gives '1' then at i =2, definitely gives '0', which implies that $\delta_{i,1}\delta_{i,2} = (1)(0) = 0$. Using this property of Kronecker deltas, Eq. (3.35) reduces into following equation. It should be noted that only underline terms of above equation survives.

$$\begin{aligned}\langle\varphi|\Phi\rangle\langle\Phi|\varphi\rangle &= \frac{1}{d}[a\alpha^2\delta_{1,k+l}\delta_{0,i+j-1}\delta_{k+l,1}\delta_{i+j-1,0} + b\alpha^2\delta_{1,k+l-1}\delta_{0,i+j}\delta_{k+l-1,1}\delta_{i+j,0}\\ &+c\alpha\beta\delta_{1,k+l}\delta_{0,i+j-1}\delta_{k+l-1,0}\delta_{i+j,1} + c\alpha\beta\delta_{0,k+l-1}\delta_{1,i+j}\delta_{k+l,1}\delta_{i+j-1,0}\\ &+a\beta^2\delta_{0,k+l}\delta_{1,i+j-1}\delta_{k+l,0}\delta_{i+j-1,1} + b\beta^2\delta_{0,k+l-1}\delta_{1,i+j}\delta_{k+l-1,0}\delta_{i+j,1}]. \end{aligned}$$

Rearranging above equation.

$$\langle\varphi|\Phi\rangle\langle\Phi|\varphi\rangle = \frac{1}{d}[a\beta^2\delta_{k+l,0}\delta_{i+j,2} + b\alpha^2\delta_{k+l,2}\delta_{i+j,0} + (a\alpha^2 + b\beta^2 + 2c\alpha\beta)\delta_{k+l,1}\delta_{i+j,1}]. \tag{3.37}$$

Putting value of Eq. (3.37) into Eq. (3.26)

$$\begin{aligned} F^{qrst} = & (\sum_{ikjl} P^{qrst}_{ikjl}\frac{a\beta^2}{d}\delta_{k+l,0}\delta_{i+j,2} + \sum_{ikjl} P^{qrst}_{ikjl}\frac{b\alpha^2}{d}\delta_{k+l,2}\delta_{i+j,0} \\ & + \sum_{ikjl} P^{qrst}_{ikjl}\frac{(a\alpha^2 + b\beta^2 + 2c\alpha\beta)}{d}\delta_{i+j,1}\delta_{k+l,1})^{\frac{1}{2}}. \end{aligned} \tag{3.38}$$

Now looking at Eq. (3.38), we have three terms with different Kronecker deltas 'δ'. In following calculation *a, b, c* and *d* are the coefficient which we calculated by using Eqs. (3.28), (3.29), (3.30), and (3.32) respectively.

First term: When $i + j = 2$ and $k + l = 0$, then the first term of Eq. (3.38) survived. Therefore first term gives us

$$\text{First term} = \beta^2(P^{qrst}_{2000} + P^{qrst}_{0020}). \tag{3.39}$$

Second term: When $i + j = 0$ and $k + l = 2$, then the second term of Eq. (3.38) survived . Thus second term gives

$$\text{Second term} = \alpha^2(P^{qrst}_{0200} + P^{qrst}_{0002}). \tag{3.40}$$

Similarly for

Third term: When $i + j = 1$ and $k + l = 1$, then the third term of Eq. (3.38) survived. So third term is given as

$$\text{Third term} = (\alpha^2 + \beta^2)^2P^{qrst}_{1100} + (\alpha^2 + \beta^2)^2P^{qrst}_{0011} + (\alpha^2 - \beta^2)^2P^{qrst}_{1001} + (\alpha^2 - \beta^2)^2P^{qrst}_{0110}.$$

Since we know that $\alpha^2 + \beta^2 = 1$, therefore

$$\text{Third term} = P^{qrst}_{1100} + P^{qrst}_{0011} + (\alpha^2 - \beta^2)^2(P^{qrst}_{1001} + P^{qrst}_{0110}). \tag{3.41}$$

Finally putting values from Eqs. (3.39), (3.40), and (3.41) into Eq. (3.38)

$$F^{qrst} = [\beta^2(P^{qrst}_{2000} + P^{qrst}_{0020}) + \alpha^2(P^{qrst}_{0200} + P^{qrst}_{0002}) + P^{qrst}_{1100} + P^{qrst}_{0011} + (\alpha^2 - \beta^2)^2(P^{qrst}_{1001} + P^{qrst}_{0110})]^{\frac{1}{2}}. \quad (3.42)$$

We are going to use Eq. (3.23) to find out different P^{qrst}_{ikjl},
Therefore

$$P^{qrst}_{2000} + P^{qrst}_{0020} = \frac{\alpha^2[\tanh^4\chi]}{2 \times Z^{qrst}}(p(qrst|2000) + p(qrst|0020)), \quad (3.43)$$

$$P^{qrst}_{0200} + P^{qrst}_{0002} = \frac{\beta^2[\tanh^4\chi]}{2 \times Z^{qrst}}(p(qrst|0200) + p(qrst|0002)), \quad (3.44)$$

$$P^{qrst}_{1100} + P^{qrst}_{0011} = \frac{[\tanh^4\chi]}{4 \times Z^{qrst}}(p(qrst|1100) + p(qrst|0011)), \quad (3.45)$$

$$P^{qrst}_{0110} + P^{qrst}_{1001} = \frac{[\tanh^4\chi]}{4 \times Z^{qrst}}(p(qrst|0110) + p(qrst|1001)). \quad (3.46)$$

Thus Eq. (3.42) becomes

$$F^{qrst} = \Big[\frac{\tanh^4\chi}{2 \times Z^{qrst}}\{\alpha^2\beta^2(p(qrst|2000) + p(qrst|0020) + p(qrst|0200) + p(qrst|0002) + \frac{1}{2}(p(qrst|1100) + p(qrst|0011) + (\alpha^2 - \beta^2)^2(p(qrst|1001) + p(qrst|0110)\}\Big]^{\frac{1}{2}}. \quad (3.47)$$

It should be noted that $p(qrst|ikjl)$ are conditional probabilities of detecting photons by four threshold detectors and value of 'Z^{qrst}' is given by Eq. (3.24). Since all four detectors used in our theory of Bell state measurement are independent of each other, so $p(qrst|ikjl)$ can be written as

$$p(qrst|ikjl) = p(q|i)p(r|k)p(s|j)p(t|l). \quad (3.48)$$

Conditional probabilities $p(q|i)$, are given by Eq. (2.81) if $q = 0$ and Eq. (2.82) for $q \neq 0$. We use Eq. (3.47) to evaluate fidelity and present our results in the next chapter.

Chapter 4

Discussion of Results

We have developed a mathematical formalism for practical quantum teleportation in chapter 3 using non perturbative approach. We derived an equation for fidelity (It is the overlap or inner product of teleported mixed state and the state we want to teleport) given in Eq. (3.47), which shows the dependence of fidelity on different practical parameters like photon pair generation rate of source (χ), detectors efficiency (η) and dark counts probability ($\wp_{dc}$). In ideal scenario where the channel loss and all other losses are zero, then the fidelity will be equal to 1 because in this case the teleported state and the initial state we want to teleport will be exactly same. Thus the according to quantum mechanics the the inner product of any normalized state with itself yield one. Since we used entangled photons as a quantum channel, which were shared between Aalia and Babar before teleporting an unknown quantum state. Therefore maximum the correlation between entangled photons, higher is the probability of teleporting unknown quantum state, means that if we draw fidelity versus photon pair generation rate χ, then fidelity must be maximum in the region of χ, where entangled state is generated with very low probability of having higher order terms. It should be noted that to have maximum success of teleportation, Babar must have the photon which is entangled with Aalia's photon. Furthermore for higher values of χ, where our source generated higher order entangled states, the fidelity must decreases because in case, if two or more entangled photon pairs were generated in spatial modes i.e., 'b', 'c' and 'e', 'f', in which photons in modes 'b' and 'e' were in Aalia's lab and 'c' and 'f' were in Babar's lab, then we don't know for sure that which particle of entangled photon pair were passes through beam splitter with unknown quantum state in Bell state analyzer. Suppose that photon in mode 'b' and unknown quantum state in Aalia's lab are detected through Bell state analyzer. Since Babar has two photons in mode 'c' and 'f', if Babar measures photon in mode 'c', then teleportation is successful but

if he measures photon in mode 'f', teleportation fails because photons in spatial modes 'b' and 'f' were not entangled and we know that entanglement is the unique feature by which teleportation is possible. So for two multi pair there is half probability of success of teleportation, therefore higher the multi pair contribution the lower will be the success probability of teleportation. We present our results of effect of various parameters on fidelity in Sec. 4.1. In Sec. 4.2 we compare the fidelity obtained by our model with a a recently performed experiment [8] of quantum teleportation and find close agreement with it.

4.1 Variation of Fidelity with Various Parameters

We present our simulation of fidelity and effect of varying experimental parameters on fidelity. The source brightness or efficiency has most profound effect on fidelity. It is important to note that by increasing value of χ, the entangled photon pair generation rate, thus increase generation of entangled photon pairs and thus decreasing the probability of success of quantum teleportation, leads to low fidelity value of teleported state. Also dark counts are the fictitious photons, so some time instead of original photons, detectors detects these fictitious photons, thus leads to decreasing the success of quantum teleportation. So by increasing dark counts probability fidelity must decreases. Finally to achieve quantum teleportation with higher success, photon detectors must be highly efficient. So in our case fidelity of quantum state must increase with increasing efficiency of detectors. We present in this chapter, different graphs of fidelity versus photon pair production rate keeping one practical parameter constant between detector efficiency (η) and dark counts probability ($\wp_{dc}$) and vary the second one. Putting values from Eqs. (2.81) and (2.82) into above Eq. (3.48) to find out values of different $p(qrst|ikjl)$. Then using these values obtained from Eq. (3.48) together with Eq. (3.24) in Eq. (3.47) to find out fidelity of teleported quantum state in terms of detectors efficiency (η), dark count probability ($\wp_{dc}$) and entangled photon pair production probability (χ).

Figs. 4.1-4.8 reveal the behavior of the fidelity as a function of the photon-pair production rate χ for varying detector efficiencies and dark-count probabilities.

Fig. 4.1 shows that fidelity of telported quantum state with respect to state $|\varphi\rangle = |\pm\rangle$ versus photon pair production rate (χ) for different values of detector efficiencies and fixed dark count probability $\wp_{dc} = 1 \times 10^{-6}$. Which shows that fidelity first increases and then decreases with increasing pair production rate (χ). Also fidelity at small value of χ, increases prominently for increasing value of detectors efficiency. At higher values of pair production rate, the fidelity has approximately same values for different detectors efficiencies because at this range the effect of higher order pair production of entangled

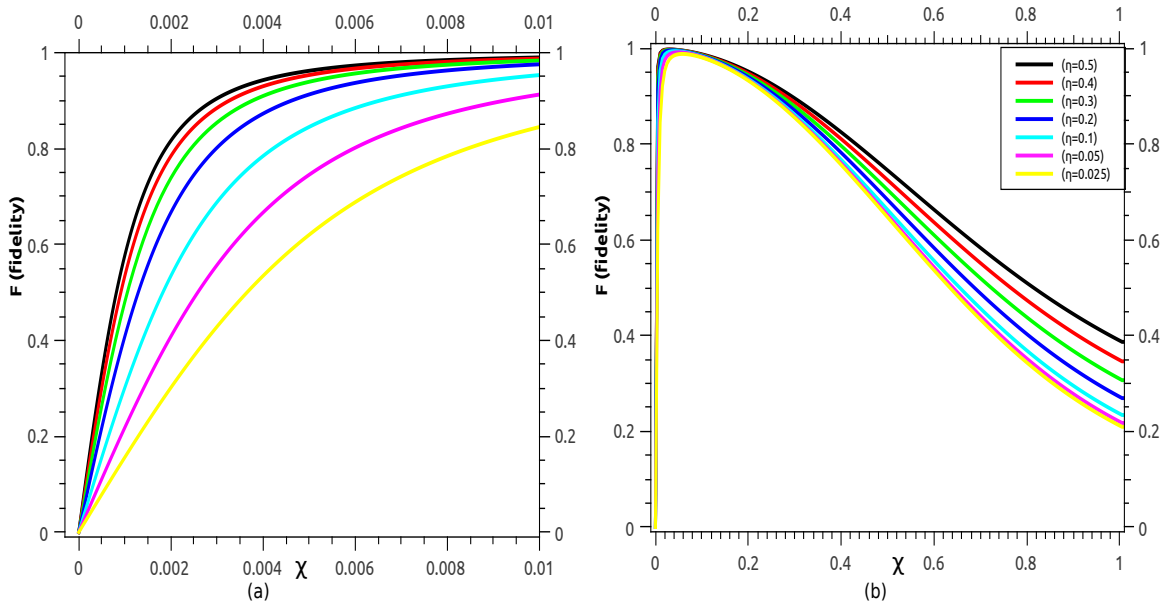

Figure 4.1: Fidelity F versus the photon-pair production rate for different detector efficiencies η for (a) Small values of χ and (b) Large values of χ. The dark-count probability is $\wp_{dc} = 1 \times 10^{-6}$ and $\alpha = 0.707, \beta = 0.707$. The function F is plotted for six different detectors efficiency values: η =0.025, 0.05, 0.1, 0.2, 0.3, 0.4, corresponding, respectively, to the curves of lowest to highest fidelity.

photons dominated all other factors.

Fig. 4.2 shows that fidelity of telported quantum state with respect to state $|\varphi\rangle = |0\rangle$ versus photon pair production rate (χ) for different values of dark count probability $\wp_{dc}$ and fixed detector efficiency $\eta = 0.2$, which shows that fidelity first increases and then decreases with increasing pair production rate (χ). In addition, fidelity at small value of χ, decreased prominently for increasing value of dark counts probabilities. This is because with high dark count probability most of the detected events are of dark counts. At higher values of pair production rate, the fidelity has approximately same values for different detectors efficiencies because at this range the effect of higher order pair production of entangled photons dominated all other factors.

Figs. 4.3 and 4.4 represents the behavior of fidelity of teleported state $|\varphi\rangle = \frac{1}{\sqrt{2}}(|0\rangle + |1\rangle)$, with $\alpha = \beta = 0.707$. In Fig. 4.3 and Fig. 4.4, we plot fidelity against photons pair production rate (χ) with fixed value of detector efficiency $\eta = 0.1$ and $\eta = 0.3$, and

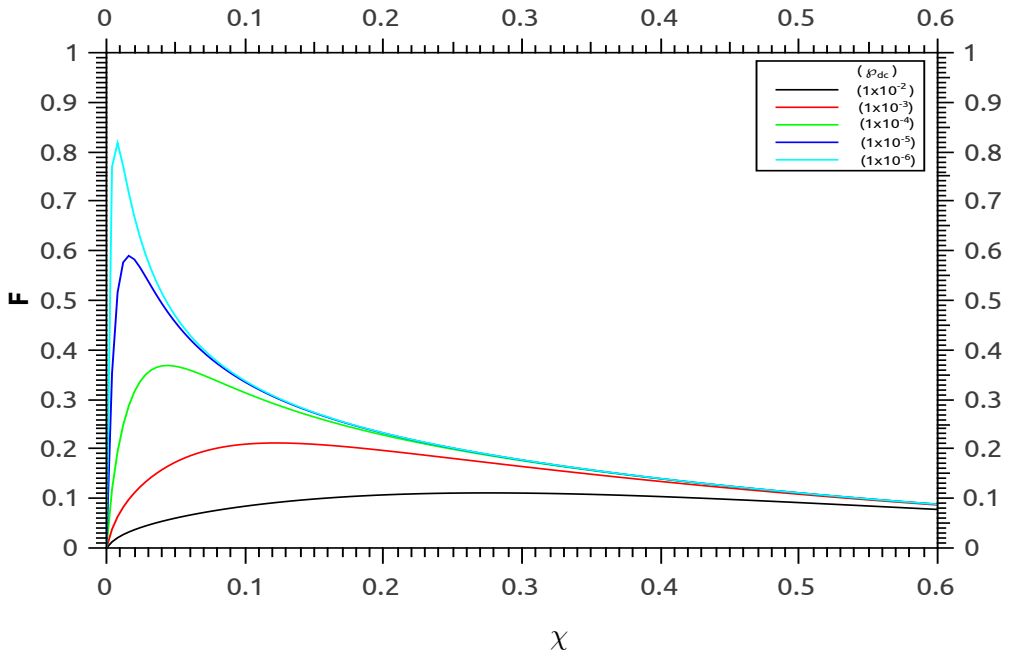

Figure 4.2: Fidelity F versus the photon-pair production rate χ for various detector dark-count probabilities and the fixed efficiency $\eta = 0.2$ and $\alpha = 1, \beta = 0$. Plots of the function F are shown for five different dark-count probabilities of detector: $\wp_{dc} = 1 \times 10^{-2}, 1 \times 10^{-3}, 1 \times 10^{-4}, 1 \times 10^{-5}, 1 \times 10^{-6}$, corresponding, respectively, to the curves of lowest to highest Fidelity .

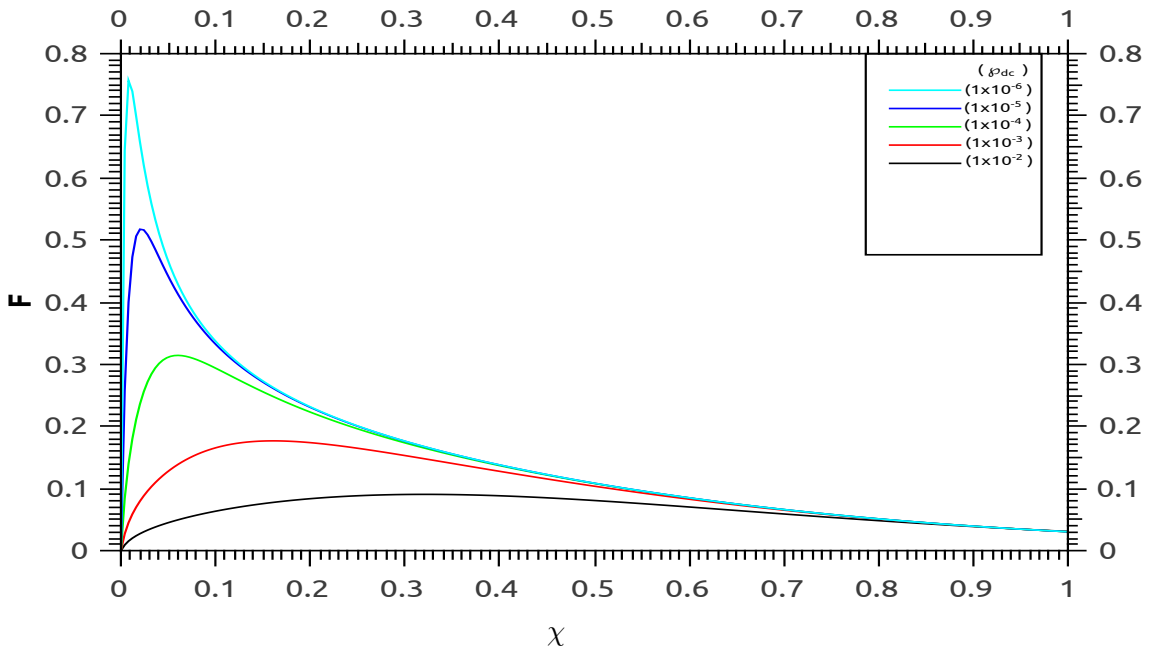

Figure 4.3: Fidelity F versus the photon-pair production rate χ for various detector dark-count probabilities and the fixed efficiency $\eta = 0.1$ and $\alpha = 0.707, \beta = 0.707$. Plots of the function F are shown for five different detector dark-count probabilities: $\wp_{dc} = 1 \times 10^{-2}, 1 \times 10^{-3}, 1 \times 10^{-4}, 1 \times 10^{-5}, 1 \times 10^{-6}$, corresponding, respectively, to the curves of lowest to highest Fidelity .

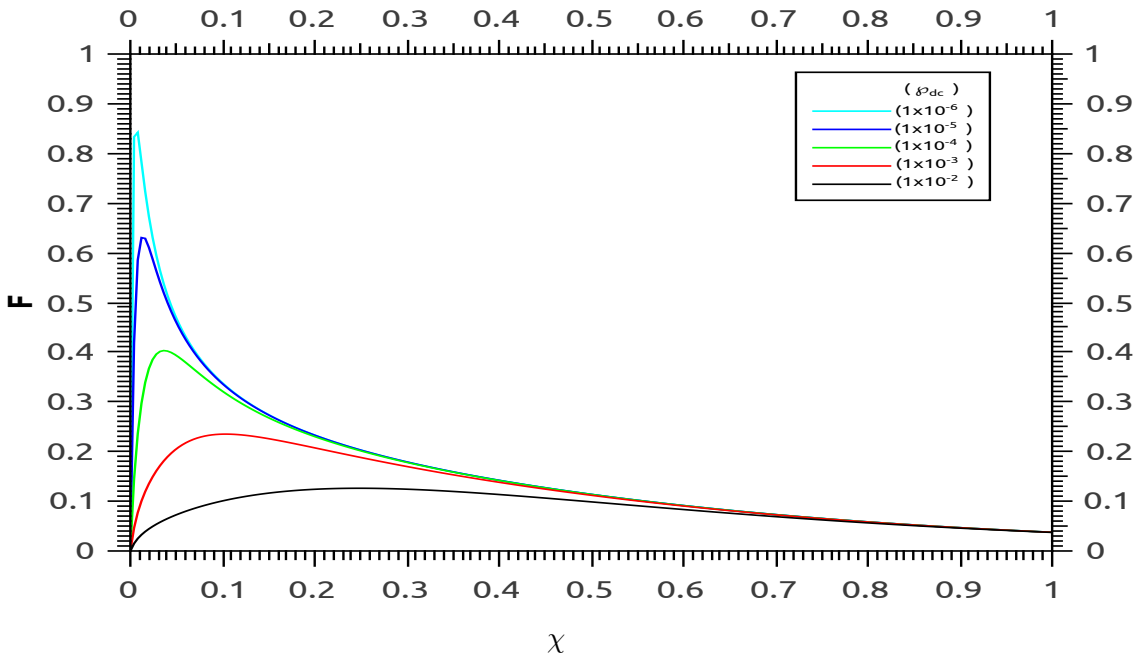

Figure 4.4: Fidelity F versus the photon-pair production rate χ for various detector dark-count probabilities and the fixed efficiency $\eta = 0.3$ and $\alpha = 0.707, \beta = 0.707$. Plots of the function F are shown for five different detector dark-count probabilities: $\wp_{dc} = 1 \times 10^{-2}, 1 \times 10^{-3}, 1 \times 10^{-4}, 1 \times 10^{-5}, 1 \times 10^{-6}$, corresponding, respectively, to the curves of lowest to highest Fidelity .

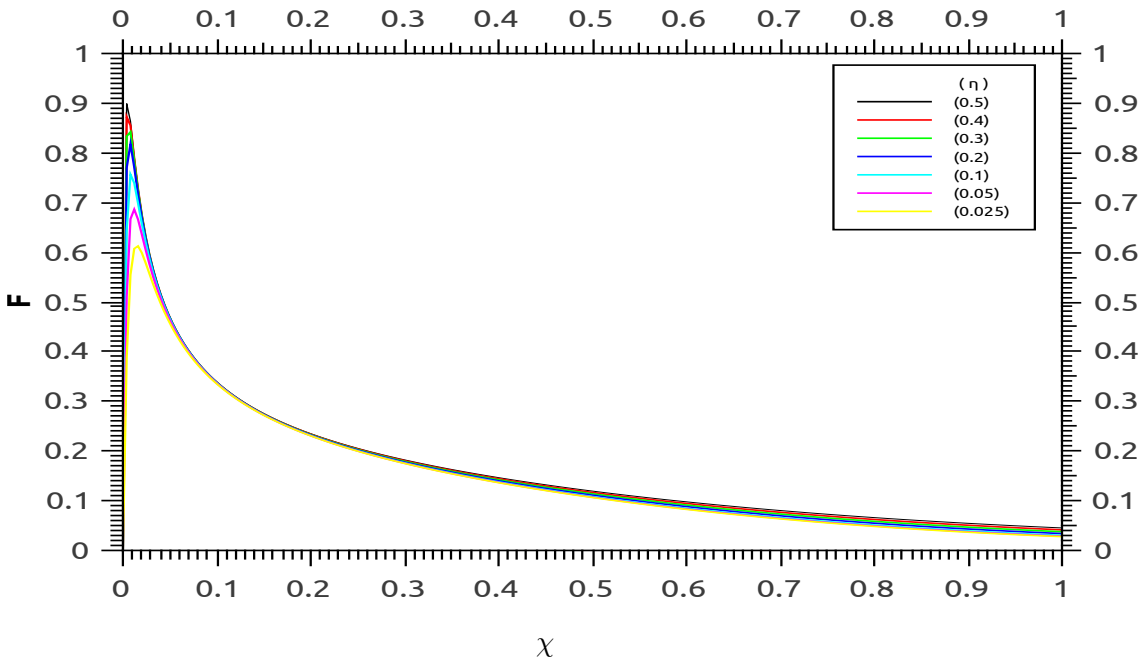

Figure 4.5: Fidelity F versus the photon-pair production rate for various detector efficiencies η and the fixed dark-count probability $\wp_{dc} = 1 \times 10^{-6}$ and $\alpha = 0.0, \beta = 1.0$. The function F is plotted for seven different detectors efficiency values: η =0.025, 0.05, 0.1, 0.2, 0.3, 0.4, 0.5 corresponding, respectively, to the curves of lowest to highest fidelity.

different dark counts probabilities respectively. In Fig. 4.5 we draw fidelity of same state used in Figs. 4.3 and 4.4 with constant dark counts probability $\wp_{dc} = 1 \times 10^{-6}$ and varying photon detectors efficiencies against photon pair production rate (χ).

It should be noted from Figs. 4.1 and 4.5 that we can teleport both quantum state $|\varphi\rangle = |0\rangle$ and $|\varphi\rangle = \frac{1}{\sqrt{2}}(|0\rangle + |1\rangle)$ with equal fidelity. So for both quantum states we got round about 82 % fidelity using detector efficienciy ($\eta = 0.2$) and dark counts probability ($\wp_{dc} = 1 \times 10^{-6}$).

Figs. 4.7 and 4.8 shows that for increasing dark counts probability $\wp_{dc}$, no matter how efficient our detectors were, the telportation scheme fails because for higher dark counts probability, the fidelity we got in Fig. 4.8 is far less than the classical limit 0.66 [34]. Therefore to perform quantum teleportation process with high success probability, we have to keep the dark counts probability less than approximately 1×10^{-4}.

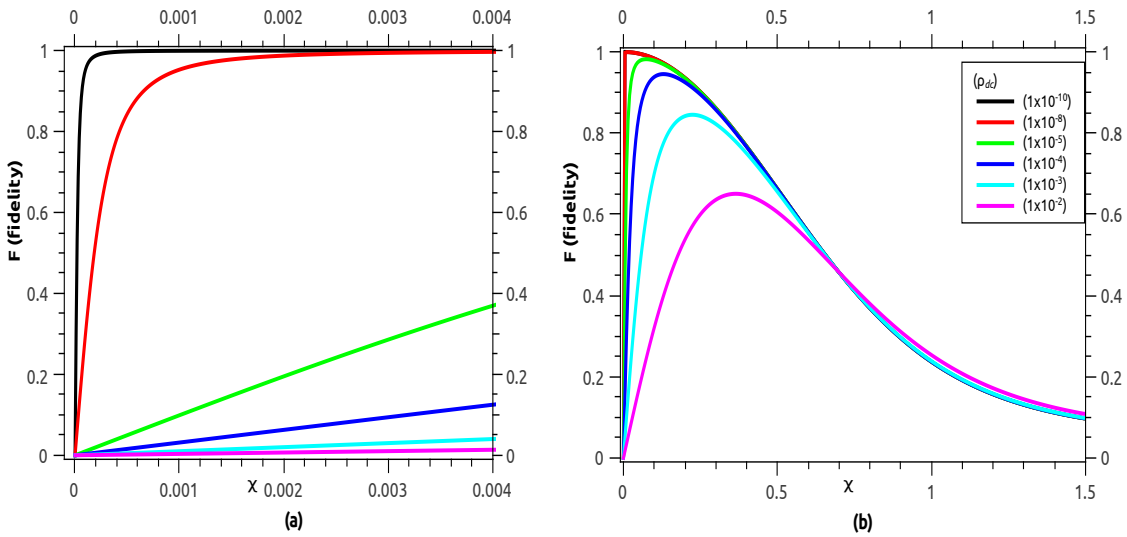

Figure 4.6: Fidelity F versus the photon-pair production rate χ for various detector dark-count probabilities for (a) Small values of χ and (b) Large values of χ. The detector efficiency is $\eta = 0.1$ and $\alpha = 0.707, \beta = 0.707$. Plots of the function F are shown for five different detector dark-count probabilities: $\wp_{dc} = 1 \times 10^{-2}, 1 \times 10^{-3}, 1 \times 10^{-4}, 1 \times 10^{-5}, 1 \times 10^{-8}, 1 \times 10^{-10}$, corresponding, respectively, to the curves of lowest to highest Fidelity .

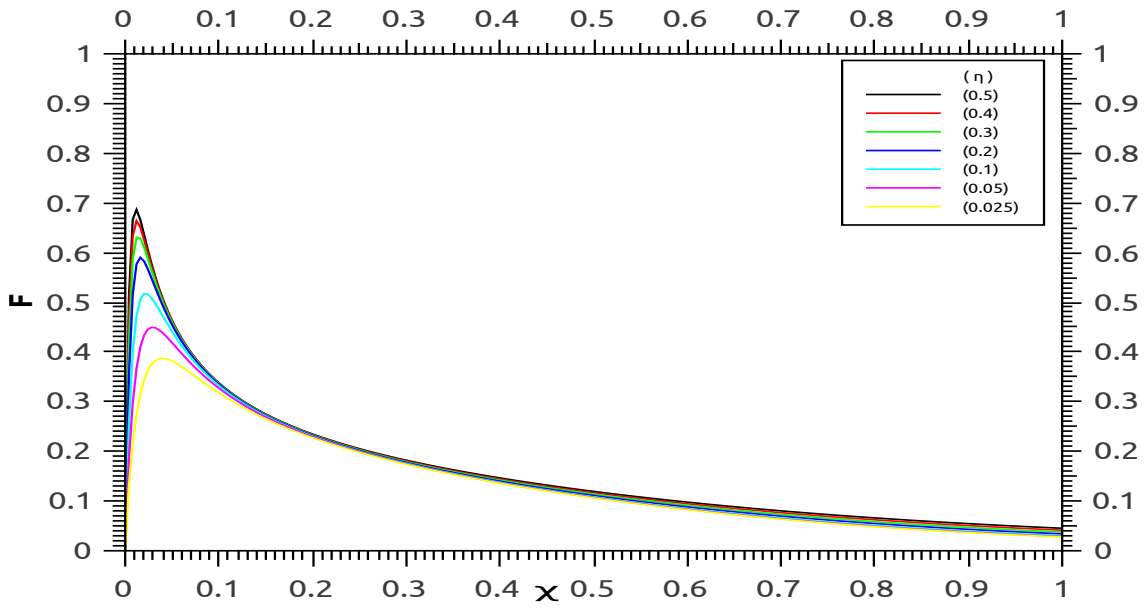

Figure 4.7: Fidelity F versus the photon-pair production rate for various detector efficiencies η and the fixed dark-count probability $\wp_{dc} = 1 \times 10^{-5}$ and $\alpha = 0.707, \beta = 0.707$. The function F is plotted for seven different detectors efficiency values: η =0.025, 0.05, 0.1, 0.2, 0.3, 0.4, 0.5 corresponding, respectively, to the curves of lowest to highest fidelity.

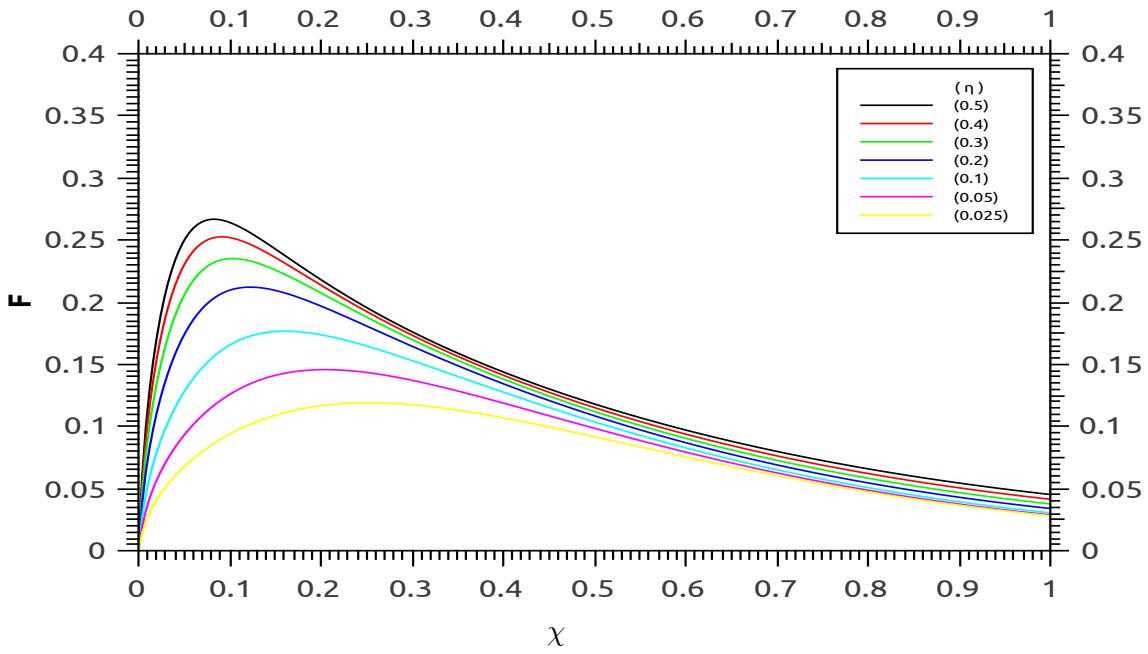

Figure 4.8: Fidelity F versus the photon-pair production rate for various detector efficiencies η and the fixed dark-count probability $\wp_{dc} = 1 \times 10^{-3}$ and $\alpha = 0.707, \beta = 0.707$. The function F is plotted for seven different detectors efficiency values: η =0.025, 0.05, 0.1, 0.2, 0.3, 0.4, 0.5 corresponding, respectively, to the curves of lowest to highest fidelity.

4.2 Applying Our Model to a Quantum Teleportation Experiment:

In order to test the validity of our theory of quantum teleportation with experimental quantum teleportation, we have to use the same values of practical parameter such as photon pair production rate, χ, detectors efficiency η and dark counts as used in experiment. It is important to note that in our theory transmission efficiency is included in detection efficiency.

We compare the predictions of our theory with a recent experiment of quantum teleportation using polarization property of photons [8], in which all required parameters related to dark counts, photon pair production rate and loss of transmission as well as detectors, are given explicitly. The conditions of this experiment are given by approximate values: detectors efficiency $\eta \approx 0.236$, transmission line has loss coefficient 45 dB, $\chi \approx \sqrt{0.1} \approx 0.316$ and dark counts $200s^{-1}$. Fig. 4.9 demonstrate, our numerical simulation result of fidelity using parameters, used in experimental quantum teleportation paper [8]. In our case the average fidelity amounts to be 82%, where the average fidelity obtained by experiment is 81.35% with ± 1 standard deviation.

Fig. 4.9 shows the behavior of the fidelity as a function of the square root of the photon-pair production rate χ for detector efficiencies and dark-count probabilities chosen as according to experiment [8]. It is interesting to observe that the photon-pair production rate of the PDC sources used in this experiment, $\chi \approx 0.316$, lies far beyond its optimal value. The small difference in both average fidelities, we believe is that the detectors inefficiency and multi-photon pair production are not the only practical limitation that effect the fidelity. Other limitations includes the imperfect entanglement generated by source, even in the scenario where only one single pair is created.

We now want to check the main limiting parameter in our teleportation theory, therefore we plot fidelity against square root of photon pair production rate χ, for fixed and small value of dark counts probability $\wp_{dc} = 0.6 \times 10^{-10}$ and different detectors efficiencies as shown in Fig. 4.11. From Fig. 4.11 it is clear that above the classical limit, fidelity does not change prominently with changing detectors efficiencies. It should be noted that there is region for some small value of χ, shows that we can achieve unit fidelity irrespective of detectors efficiencies. Fig. 4.10, shows how fidelity varies for fixed $\wp_{dc}$ and different detectors efficiencies in region of very small values of χ.

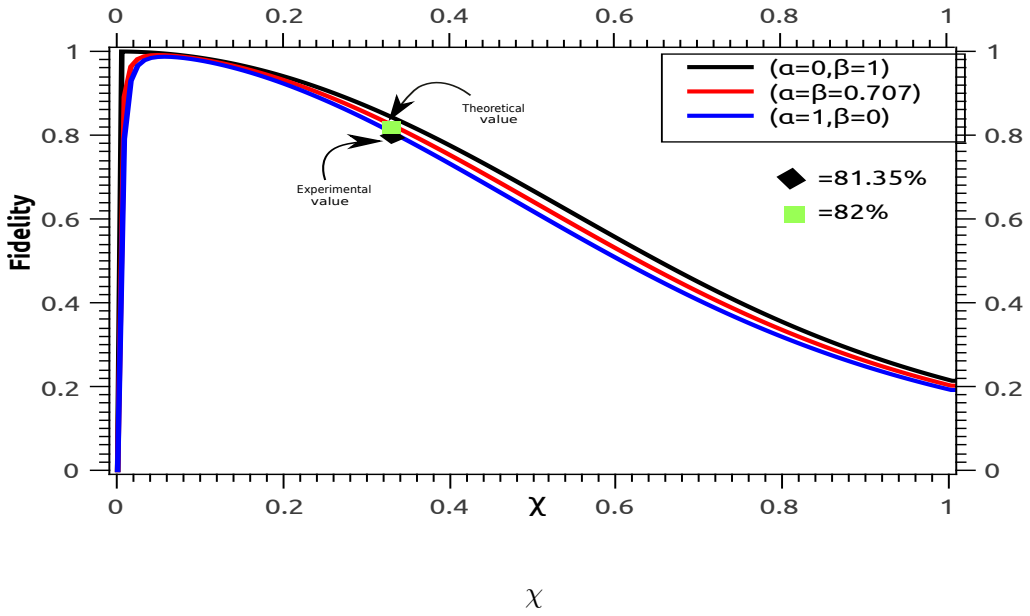

Figure 4.9: Fidelity F versus the square root of photon-pair production rate with fixed dark-count probability $\wp_{dc} = 0.6 \times 10^{-10}$ and same detectors efficiency value: $\eta = 0.7463 \times 10^{-5}$ includes transmission losses, for different initial quantum states: $|0\rangle$, $|\pm\rangle$, and $|1\rangle$ corresponding, respectively, to the curves of lowest to highest fidelity. We obtained average fidelity 82%.

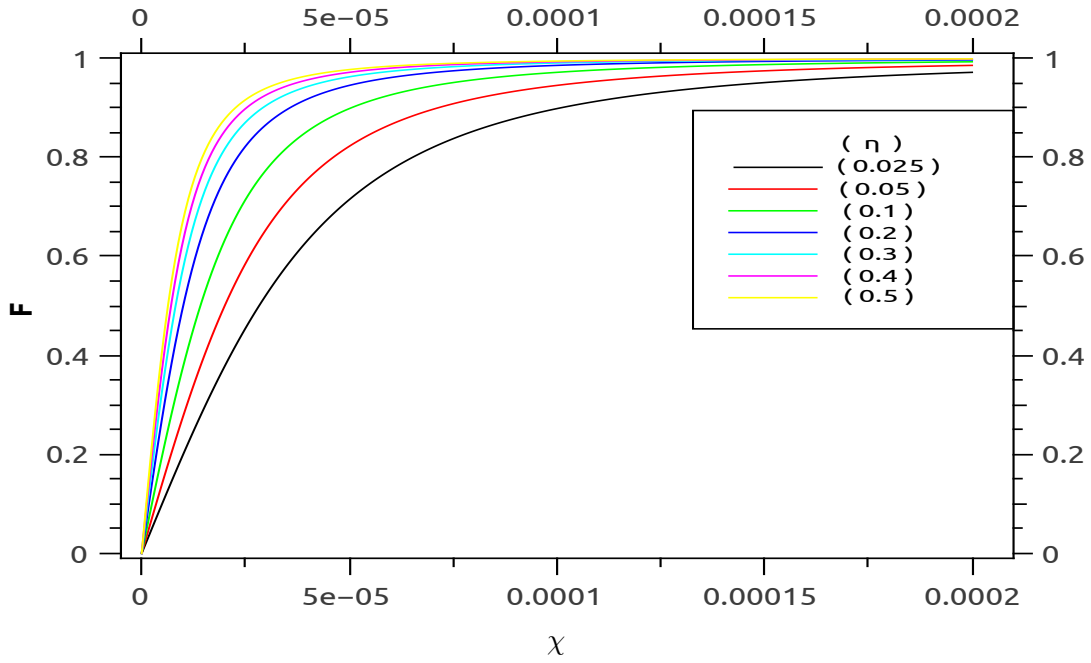

Figure 4.10: Plot of fidelity F against the photon-pair production rate χ for the fixed dark-count probability $\wp_{dc} = 0.6 \times 10^{-10}$ and different detectors efficiency value: $\eta = 0.025, 0.05, 0.1, 0.2, 0.3, 0.4, 0.5$, for quantum states: $|\pm\rangle$, having $\alpha = \beta = 0.707$ corresponding, respectively, to the curves of lowest to highest fidelity.

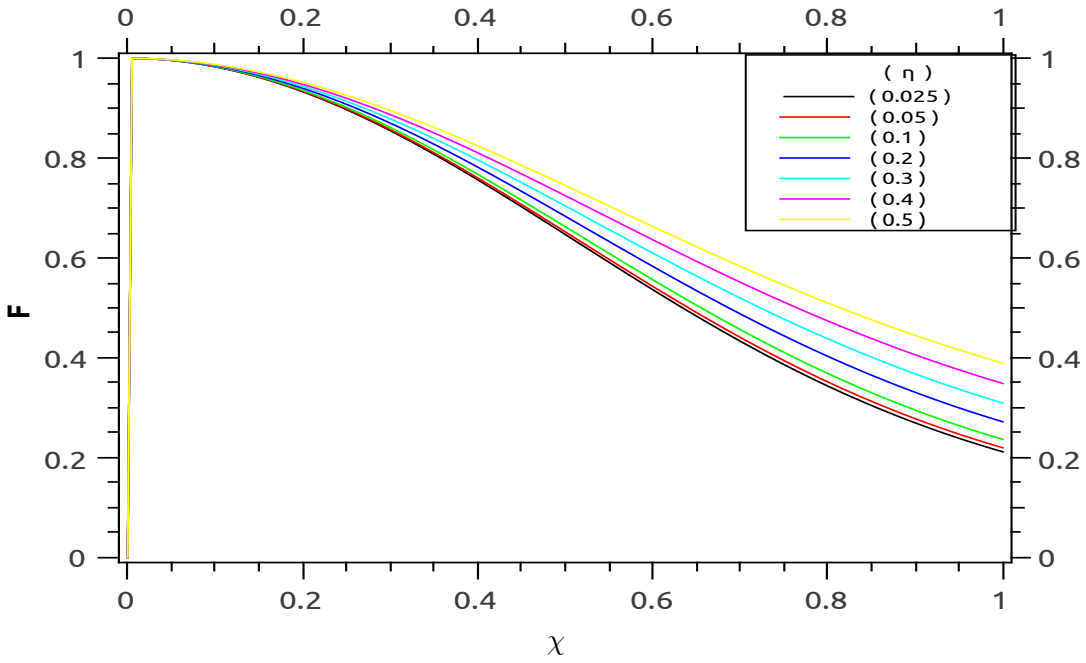

Figure 4.11: Plot of fidelity F against the photon-pair production rate for χ the fixed dark-count probability $\wp_{dc} = 0.6 \times 10^{-10}$ and different detectors efficiency value: $\eta = 0.025, 0.05, 0.1, 0.2, 0.3, 0.4, 0.5$, for quantum states: $|\pm\rangle$, having $\alpha = \beta = 0.707$ corresponding, respectively, to the curves of lowest to highest fidelity.

Chapter 5

Conclusion

5.1 Sources and Detectors

In this dissertation we studied perfect sources of generation of entangled photons pair as well as ideal detectors for detecting these photons. In addition, in our theory we focused on non-ideal sources and photons detectors because technological it is impossible to produce a single entangle photon pair on demand and to detect single photons. We used PDC source to produce entangled photon pair which are completely probabilistic in nature. This probabilistic nature or randomness of production of entangled photon pair is shown in Eq. (2.15) by vacuum part as

$$Z(\gamma) = |\text{vac}\rangle + \frac{i\gamma}{2}|1010\rangle, \qquad \gamma \in R. \tag{5.1}$$

which, shows that when laser pulse is allowed to pass through a BBO crystal, it well either be converted into entangled photon pair or pass without converting into entangle pair. Thus the vacuum component in above equation shows that there is maximum possibility that PDC will not take place. It should be noted that the rate of generation of entangled photon pair is proportional to nonlinearity $\chi^{(2)}$ of the crystal, the interaction time and the strength of the pump laser. Now to over come the problem of randomness of generation of entangled photon pair we can either use crystal with high nonlinearity $\chi^{(2)}$ or stronger laser pump pulses. But by doing so we come across with a consequence of generation of multi-pairs of entangled photons, which must be avoided as far as possible because such events effects the experiments. It should be kept in mind that we cannot exclude the probability of multi pair emission. On the other hand if we take crystal with small value of nonlinearity $\chi^{(2)}$, gives strong component of vacuum which show that most of time PDC

did not happened. So taking crystal either with larger or small value of nonlinearity $\chi^{(2)}$ will effect experiment.

Then we discuss the theoretical model of different detectors. In our theory we have used detectors which click when there is at least one photon and do not click if there is no photon present in the incoming mode. These detectors do not differentiate between one photon or more. Such detectors are called *threshold detectors*. We also discussed the model of photon number discriminating detectors which can effectively differentiate between one photon and more. Then for both type of detectors we calculated conditional probabilities of detecting photons.

5.2 Practical Quantum Teleportation

We have developed the theory of practical quantum teleportation. We have first calculated the quantum state produced by SPDC TYPE-II source given in Eq. (2.35). Then we find out the quantum state of teleported photon. Using ideal photon number discriminating detectors we find out hypothetical probability given in Eq. (3.18). Taking advantage of Bayesian inference we then calculate the probability of detecting photons for faulty detectors. At last we have calculated fidelity, a very important property of quantum states which shows how much two quantum state are similar, in terms of nonlinearity, $\chi^{(2)}$, of BBO crystal, detectors efficiency η and dark counts probability $\wp_{dc}$. We then show the variation of fidelity with the photon pair production rate, χ, while fixing either dark counts, $\wp_{dc}$, and varying detectors efficiency, η, or vise versa. Our theory gives very good results, which tells us that fidelity increases when we increase the efficiency η of detectors while keeping dark counts probability constant. On the other hand fidelity decreases when we increase the probability of dark counts $\wp_{dc}$ while keeping the detector efficiency η fixed. Also by increasing photon pair production rate χ, fidelity first increasing and then decreasing as shown in Figs. 4.1-4.11. This dependence is due to that for small value of χ the probability of photon pair generation is small and thus fidelity obtained is small because we do not have entangled photon pair due to vacuum component, but as soon χ reached certain value which generate entangled photon pair with very less multi pair photons generation our fidelity reaches certain maximum value which is far greater than classical value 0.66 [34]. A very valuable conclusion we get from our investigation that the high photon pair production rate is counterproductive. If we exceed value of χ, after certain value of $\chi = 6 \times 10^{-2}$, fidelity starts decreasing After further increasing χ the fidelity decreased because of the events due multi pair photon generation.

We test our theory against experimental quantum teleortation [8], i.e., using same practical parameters given in [8], we obtained average fidelity of 82%. Our calculated

fidelity is in good agreement with the experimental value. Thus our model fits very well to the real world experimental conditions. Our model can be used to predict the optimal parameters for the resources used to get the desired fidelity.

Bibliography

[1] C. H. Bennett and G. Brassard, *Quantum Cryptography: Public Key Distribution and Coin Tossing*, Proc. IEEE International Conferrecne on Computers, systems and Signal Processing, (Bangalore, India), 175 (1984).

[2] C. H. Bennett, G. Brassard, C. Crepeau, R. Jozsa, A. Peres and W. K. Wootters *Teleporting an Unknown Quantum State via Dual Classical and Einstein-Podolsky-Rosen Channels*, Phys. Rev. Lett. **70**, 1895 (1993).

[3] C. H. Bennett and S. J. Wiesner, *Communication via one- and two-particle operators on Einstein-Podolsky-Rosen states* Phys. Rev. Lett. **69**, 2881 (1992).

[4] C. H. Bennett, D. P. Divincenzo, J. A. Smolin , W. K. Wootters, *Mixed-state entanglement and quantum error correction*, Phys. Rev. A, **54**, 3824 (1996).

[5] A. K. Ekert, *Quantum cryptography based on Bell's theorem*, Phys. Rev. Lett., **67**, 661 (1991) .

[6] C. H. Bennett and J. Smolin, *Experimental quantum cryptography*, J. Cryptology, **5**, 3 (1992)

[7] D. Bouwmeester, J. W. Pan, K. Mattle, M. Eibl, H. Weinfurter and A. Zeilinger, *Experimental quantum teleportation*, Nature **390**, 575 (1997).

[8] J. Yin, J. G. Ren, H. Lu, Y. Cao,H. L. Yong, Y. P. Wu, C. Liu, S. K. Liao, F. Zhou, Y. Jiang, X. D. Cai, P. Xu, G. S. Pan, J. J. Jia, Y. M. Huang, H. Yin, J. Y. Wang, Y. A. Chen, C. Z. Peng, and J. W. Pan , *Quantum teleportation and entanglement distribution over 100-kilometre free-space channels*, Nature **488**, 185 (2012).

[9] R. P. Feynman, R. B. Leighton, and M. Sands, *The Feynman Lectures of Physics*, Quantum Mechanics, Addison-Wesley, Reading, **HI** (1965).

[10] G. L. Taylor, *Interference Fringes with Feeble Light* Proc. Camb. Phil. **15**, 114 (1909).

[11] A. Zeilinger, R. Gaehler, C. G. Shull, W. Treimer, W. Mampe, *Single and Double Slit Diffraction of Neutrons*, Rev. Mod. Phys. **60**, 1988.

[12] O. Carnal and J. Mlynek, *Young's double-slit experiment with atoms: A simple atom interferometer* Phys. Rev. Lett. **66**, 2689 (1991).

[13] G. Mollenstedt and G. Jonsson, *Some remarks on the quantum mechanics of the electron*, Z. Phys. **155**, 472 (1959).

[14] D. Bohm, *The Undivided Universe: An Ontological Interpretation of Quantum Theory*, Routledge; Reprint edition (1995).

[15] H. Weinfurter and A. Zeilinger, *Quantum Communication*, Springer, Berlin/ Heidelberg, **173**, 58 (2001).

[16] D. R. Truax, *Baker-Campbell-Hausdorff relations and unitarity of SU(2) and SU(1,1) squeeze operators*, Phys. Rev. **31**, 1988 (1985).

[17] B. Yurke, S. L. McCall and J. R. Klauder, *SU(2) and SU(1,1) interferometers* Phys. Rev. A **33**, 4033 (1986).

[18] S. D. Bartlett, D. A. Rice, B. C. Sanders, J. Daboul and H. de Guise, *Unitary transformations for testing Bell inequalities*, Phys. Rev. A **63**, 042310 (2001).

[19] A. Scherer, R. B. Howard, B. C. Sanders and W. Tittel, *Quantum states prepared by realistic entanglement swapping* Phys. Rev. A **80**, 062310 (2009).

[20] A. Scherer, B. C. Sanders, and W. Tittel, *Long-distance practical quantum key distribution by entanglement swapping* Vol. **19**, 4 (2011).

[21] F. Zappa, A. Lacaita, S. Cova, and P. Webb, *Nanosecond single-photon timing with InGaAs/InP photodiodes* Optics Letters, **19**, 846 (1994).

[22] S. D. Bartlett and B. C. Sanders, *Universal continuous-variable quantum computation: Requirement of optical nonlinearity for photon counting* Phys. Rev. A **65**, 042304 (2002).

[23] W. K. Wootters, W. H. Zurek, *A Single Quantum Cannot be Cloned.* Nature **299**, 802 (1982).

[24] Z. Zhao, Y. A. Chen, A. N. Zhang, T. Yang, H. J. Briegel and J. W. Pan, *Experimental demonstration of five-photon entanglement and open-destination teleportation*, Nature **430**, 54 (2004).

[25] J. W. Pan, D. Bouwmeester, H. Weinfurter and A. Zeilinger, *Experimental Entanglement Swapping: Entangling Photons That Never Interacted* Phys. Rev. Lett. **80**, 3891 (1998).

[26] Q. Zhang, A. Goebel, C. Wagenknecht, Y. A. Chen, B. Zhao, T. Yang, A. Mair, J. Schmiedmayer AND J. W. Pan, *Experimental quantum teleportation of a two-qubit composite system.* Nature Physics **2**, 678 (2006).

[27] I. Marcikic, H. de Riedmatten, W. Tittel, H. Zbinden and N. Gisin, *Long-distance teleportation of qubits at telecommunication wavelengths* Nature **421**, 509 (2003).

[28] R. Ursin, T. Jennewein, M. Aspelmeyer, R. Kaltenbaek, M. Lindenthal, P. Walther and A. Zeilinger, *Communications: Quantum teleportation across the Danube*, Nature **430**, 849 (2004).

[29] M. Aspelmeyer,H. R. Bohm, T. Gyatso, T. Jennewein, R. Kaltenbaek, M. Lindenthal, G. M. Terriza, A. Poppe, K. Resch, M. Taraba, R. Ursin, P. Walther and A. Zeilinger, *Long-Distance Free-Space Distribution of Quantum Entanglement*, Science **301**, 621 (2003).

[30] C. Z. Peng, T. Yang, X. H. Bao, J. Zhang, X. M. Jin, F. Y. Feng, B. Yang, J. Yang, J. Yin, Q. Zhang, N. Li, B. L. Tian and J. W. Pan, *Experimental Free-Space Distribution of Entangled Photon Pairs Over 13 km: Towards Satellite-Based Global Quantum Communication*, Phys. Rev. lett. **94**, 150501 (2005).

[31] R. Ursin, F. Tiefenbacher, T. S. Manderbach, H. Weier, T. Scheidl, M. Lindenthal, B. Blauensteiner, T. Jennewein, J. Perdigues, P. Trojek, B. Omer, M. Furst, M. Meyenburg, J. Rarity, Z. Sodnik, C. Barbieri, H. Weinfurter and A. Zeilinger, *Entanglement-based quantum communication over 144 km*, Nature Physics **3**, 481 (2007).

[32] A. Fedrizzi, R Ursin, T. Herbst, M. Nespoli, R. Prevedel, T. Scheidl, F. Tiefenbacher, T. Jennewein and A. Zeilinge , *High-fidelity transmission of entanglement over a high-loss free-space channel*, Nature Physics **5**, 389 (2009).

[33] X. M. Jin, J. G. Ren, B. Yang, Z. H. Yi, F. Zhou, X. F. Xu, S. K. Wang, D. Yang, Y. F. Hu, S. Jiang, T. Yang, H. Yin, K. Chen, C. Z. Peng and J. W. Pan , *Experimental free-space quantum teleportation*, Nature Photonics **4**, 376 (2010).

[34] S. Popescu, *Bell Inequalities versus Teleportation: What is Nonlocality?*, Phys. Rev. Lett. **72**, 797 (1994).